The Dissertation Committee for Tae Sang Kim Certifies that this is the approved version of the following dissertation:

Molecular Beam Studies of Low Temperature CO Oxidation on Gold

Committee:

Charles B. Mullins, Supervisor

John G. Ekerdt

Gyeong S. Hwang

Greg O. Sitz

Thomas M. Truskett

Molecular Beam Studies of Low Temperature CO Oxidation on Gold

by

Tae Sang Kim, B.S.

Dissertation

Presented to the Faculty of the Graduate School of

The University of Texas at Austin

in Partial Fulfillment

of the Requirements

for the Degree of

Doctor of Philosophy

The University of Texas at Austin

December 2005

Dedication

To Mom and Dad

Acknowledgements

I would like to thank my supervisor Dr. C. Buddie Mullins for his support, patience, and encouragement throughout my graduate studies. I greatly appreciate all the advice he has given me over the past several years and I am truly grateful for his inspiring way to guide me to become a better scientist. I also thank the other members of my committee: Dr. John G. Ekerdt, Dr. Gyeong S. Hwang, Dr. Greg O. Sitz, and Dr. Thomas M. Truskett for their suggestions on my research. I am also grateful to Dr. J. M. White for his invaluable comments on my work.

I would also like to thank my colleagues Dr. Chris Reeves and Dr. Randy Meyer for teaching me all the basics for conducting research in our lab and Dr. James Stiehl, Sean McClure, Rotimi Ojifinni, and Jinlong Gong for many interesting and good-spirited discussions relating to this research and for their friendship.

I would also like to express my gratitude to my friends outside of the lab who made my graduate school experience memorable. I thank Won Sun Ryoo, Joseph Lee, Dongman Cho, Hyug Han Kim, Pil Joong Yoon, In Sik Chin, Jungseok Hahn, Jooheon Kim, and Do Hoon Kim for their friendship and encouragement during my graduate studies.

Most importantly, I would like to thank all of my family for all the love and support that they have given me throughout my graduate school life. I especially thank my parents for their unconditional support and love throughout my early years and all the way through graduate school as I pursued this work far away from home.

Molecular Beam Studies of Low Temperature CO Oxidation on Gold

Publication No._____

Tae Sang Kim, Ph.D.

The University of Texas at Austin, 2005

Supervisor: Charles B. Mullins

Gold is considered as noble among other metals because of its resistance to oxidation and corrosion. It is the most electronegative metal and its electron affinity is actually greater than that of oxygen. For this reason gold will not react directly with other electronegative elements such as molecular oxygen. As a result, gold has not been given much attention as a potential active ingredient for heterogeneous catalysis until it was discovered that gold particles that are 2-5 nm in diameter have exceptional catalytic activity towards many reactions. Among these reactions, low temperature CO oxidation is one of the most unique regarding gold catalysts in that it cannot be matched by other metals. Although it is widely accepted that gold particles which are 2-5 nm in diameter exhibit the greatest activity in CO oxidation, there is still much debate on the nature of the active sites for these catalysts and also the details of the reaction mechanism.

Using molecular beams in conjunction with a radio frequency generated plasma jet, I have studied CO oxidation with atomically adsorbed oxygen on Au/TiO_2 and Au(111). It is shown that CO reacts readily with pre-adsorbed oxygen atoms on a

Au/TiO_2 planar model catalyst and on Au(111) to produce CO_2 even at temperatures as low as 77 K. The results presented show that gold particle size seems to have little effect on CO oxidation when oxygen adatoms are pre-adsorbed. This suggests that if reactive oxygen is primarily supplied through dissociation of oxygen molecules on the surface, the rate-limiting step in CO oxidation over gold is likely to be the dissociation of molecular oxygen.

Another notable aspect of low temperature CO oxidation is that the addition of water in the feed stream is believed to enhance the reactivity by as much as two orders of magnitude. Here, evidence is shown that water can participate in CO oxidation on Au(111) surface populated with atomic oxygen by directly supplying its oxygen to CO to form CO_2 at low temperatures. The results strongly suggest the direct involvement and promoting role of water in CO oxidation on oxygen covered Au(111).

Table of Contents

List of Figures

Chapter 1: Introduction

Heterogeneous catalysis involves the use of a catalyst in a different phase from the reactants. Most commonly, solid catalysts are used with gaseous or liquid phase reactants. Due to this nature, interfacial phenomena become very important in heterogeneous catalysis. Apart from the actual surface reaction, diffusion, adsorption, and desorption play an important role in determining the reaction rate. These additional steps make it difficult to understand the exact details of the reaction. Nevertheless, heterogeneous catalysts are used in many industrial processes due to ease of preparation (which comes from the fact that they can be formed into solid pellets), recovery, and operation.

Often times, the reactive elements of heterogeneous catalysts are composed of metals. They are the key components in catalytic reforming, cracking, oxidation, reduction, and other reactions. In order to be a satisfactory candidate for a heterogeneous catalyst, the metal has to adsorb the reactants easily so that they can participate in surface reaction, but it should not adsorb the reactant so strongly that they are irreversibly bound to the metal rather than reacting with other molecules on the surface. Another requirement for a good catalyst material is that the product molecule should desorb relatively easily from the surface, so that the reaction can continue on the surface with other reactants adsorbing on the surface.

High-quality catalytic materials are mostly found among transition metals, which include iron, nickel, and especially platinum group metals, because they typically interact

strongly enough with the reactants so that they can react on the surface but not bond to the products so strongly as to inhibit further surface reaction. A good example of a heterogeneous catalyst with platinum group metals as active ingredients, used in everyday life, is the catalytic converter installed in automobiles. Catalytic converters are mainly composed of three parts.[1] First is the catalyst support which has a ceramic honeycomb structure and the inner walls that are covered with a layer of washcoat which is typically made of aluminum oxide. This washcoat is then impregnated with active metal ingredients including Pt, Pd, Rh, and other promoter materials. Pt and Pd are responsible for oxidizing unreacted hydrocarbons and CO from the exhaust and Rh functions as a NO_x reducer. These components are incorporated into the catalytic converter using a simple classical method called impregnation, which consists of repeated dipping of the catalyst support into a solution containing a desired catalytic ingredient.

As stated, common metals used in catalysis are found among group VIII elements (Fe, Ni, platinum group metals). The secret to the catalytic reactivity of these metals lie in the optimum degree of d-band vacancy. If we look at IB metals (Cu, Ag, and Au) these have full d-bands but for Cu and Ag, owing to the relatively low ionization potentials, they can have available d-orbitals for catalytic reactions.[2] Au, despite being in the same group as Cu and Ag, turns out to be the most electronegative metal. Its electron affinity is actually greater than that of oxygen. For this reason gold does not react with other electronegative elements such as oxygen and this resistance to oxidation and corrosion is what makes gold a noble metal. Owing to being chemically inert, gold had been overlooked as a possible candidate as a catalytically active material until Haruta's seminal discovery of the exceptional reactivity of nanometer sized (2-5 nm in diameter)

gold particles nearly 20 years ago.[3] One of the reasons that so many scientists missed the high reactivity of gold catalysts is that if gold catalysts are prepared using the classical impregnation method, the size of the gold particles are much larger than that of say Pt, in which case gold becomes inactive.[4] This is partly due to the fact that the melting point of gold is much lower than other platinum group metals. In order to make small enough gold particles, the most popular method used these days is deposition-precipitation method,[5] where support powder is suspended in the metal solution and metal hydroxide precipitate on the surface of support material by raising the pH of the solution. After precipitation is complete, the solid is filtered for further treatment. Using such methods, gold particles are in the optimum size range (2-5 nm in diameter) where they exhibit exceptional reactivity.

Since the significant findings of Haruta, there has been an exponential growth in gold catalysis research. Some of the reactions studied include low temperature CO oxidation,[6-12] propylene epoxidation,[13-15] and the water gas shift reaction.[16-18] Among these reactions, low temperature CO oxidation is one of the most unique regarding gold catalysts in that it cannot be matched by other metals. This low temperature reactivity has generated great interest and much research of metal oxide supported gold nanoparticles.

The unique nature of gold to oxidize other reactants has gained much interest in the catalysis community and now it is showing great promise in many other reactions. The oxidation of alcohols is of great importance in fine chemical production and gold based catalysts have been shown to be very effective catalysts in oxidizing alcohols to acids. A good example is glycerol oxidation to glyceric acid.[19] Another example of gold catalysts exceptional reactivity is the direct synthesis of hydrogen peroxide. Hydrogen

peroxide is often used in selective oxidation reactions at ambient conditions and presently, it is only economical to produce on a large scale by sequential hydrogenation and oxidation of alkyl anthraquinone.[20] Due to the problems of transportation and storage of hydrogen peroxide, it would be advantageous if hydrogen peroxide could be produced in small scale. It has been found that gold catalysts can be very effective in producing hydrogen peroxide in a smaller scale by direct synthesis from hydrogen and oxygen.[21,22] Demonstrating another good example of gold catalysts as effective oxidation catalysts, it has been shown that gold catalysts can selectively oxidize cyclohexene to produce epoxides using molecular oxygen as an oxidant.[23] This is a great step forward from smaller alkene oxidation which demonstrates the great potential of gold based catalysts in green chemistry where hazardous intermediates can be avoided to make useful partially oxidized products. These studies indicate the possibilities for gold catalysts to be used as effective catalysts for oxidation reactions are just beginning to emerge and many other discoveries are bound to appear in the near future.

In order to understand the fundamental aspects of catalytic activity, many single crystal metals exposing a specific crystal plane were studied under ultrahigh vacuum conditions to reveal how gas molecules adsorb on surfaces and react on surfaces. The mechanism of some catalytic reactions has been clarified from experiments on single crystal metals. However, metal single crystals are unable to explain the size effect of metal particles and the metal support interaction that are present in real catalysts. These limitations can be overcome by fabricating a planar model catalyst where active metal particles are dispersed on top of well defined metal oxide supports.[24,25] Since they still retain the two dimensional structure, they can be easily characterized and tested by many

surface science techniques. Gold particles supported on TiO_2(110) have been a popular model catalyst system and this system is part of the work presented here.

Although it is widely accepted that gold particles which are 2-5 nm in diameter exhibit the greatest reactivity, there is still much debate on the nature of the active sites for these catalysts and also the details of the reaction mechanisms. While some suggest the perimeter interface of gold particles and the metal oxide support as the active site for CO oxidation,[26-29] others point to low coordination sites on small gold particles based on calculations and gas phase cluster experiments.[30-32] Another issue that is still under debate is the oxidation state of the active form of gold. Some studies state that metallic gold is the active form of gold[33,34] while others claim oxidic gold[35,36] is responsible for the reactivity of gold. One notable aspect of low temperature CO oxidation is that the addition of water in the feed stream is believed to enhance the reactivity by as much as two orders of magnitude.[37] It has been postulated that water can promote the reaction by either activating the molecular oxygen on the surface to enhance CO_2 production or help decompose the carbonates that may accumulate on the surface to accommodate additional reactants on the surface.[37,38] Both of these hypotheses propose that water is not directly participating in the reactions, but only indirectly assisting reactions.

As might be clear from these issues, there are still many questions that need to be resolved in highly active CO oxidation on gold catalysts and further research is necessary to clarify these matters. In this dissertation, an attempt is made to provide insight into the mechanistic details of the CO oxidation reaction and the role of moisture on Au/TiO_2 model catalysts and Au(111) single crystal surface.

Chapter 2 briefly shows that CO reacts readily with pre-adsorbed oxygen atoms on a Au/TiO_2 planar model catalyst to produce CO_2 even at temperatures as low as 65 K. Results are presented where gold particle size seems to have little effect on the CO oxidation reaction when oxygen adatoms are pre-adsorbed. This is in contrast to the previous studies employing molecular oxygen as a reactant in studies by Haruta and Goodman where they demonstrate a strong particle size effect in CO oxidation at ambient conditions. This suggests that if reactive oxygen is supplied mainly through dissociation of oxygen molecules on the surface, the rate-limiting step in CO oxidation over gold is likely to be the dissociation of molecular oxygen. It is also shown that as the oxygen adatom coverage increases, the rate of CO oxidation decreases on Au/TiO_2 at cryogenic temperatures.

In Chapter 3, CO oxidation on oxygen precovered Au(111) was studied as a function of oxygen coverage to understand the basic reaction mechanism on gold at a sample temperature of 77 K. Results are shown in which prompt CO_2 production was observed when the CO beam impinges on the sample followed by an exponential decay of CO_2 production in all cases. At oxygen precoverages above 0.5 ML, the initial CO_2 production was shown to decreases with increasing oxygen precoverage mainly due to the decrease in CO uptake with increasing O precoverage. The reaction mechanism of CO oxidation at 77 K is believed to be precursor mediated, in which CO is in a precursor state or trapped state and oxygen atoms are in a chemisorbed state.

Chapter 4 is a brief account of how water can promote oxidation of impinging CO molecules on oxygen atom precovered Au(111) at low temperatures. CO_2 production was seen to greatly increase with the addition of water on the same oxygen precoverage,

and it is proposed that these results are due to CO reacting directly with activated water or OH groups formed from water interacting with atomic oxygen on Au(111).

Chapter 5 deals with the details of Chapter 4 which include the interaction of water and oxygen atoms on Au(111) surface. It is shown that water interacts with oxygen atoms on the Au(111) surface resulting in oxygen scrambling on the surface. The role of metastable oxygen in water-oxygen interaction and the promotional effect of water on CO oxidation is also discussed.

In Chapter 6, major findings of this dissertation will be presented with some recommendations for future research projects.

REFERENCES

1. J. Kaspar, P. Fornasiero, N. Hickey, Catal. Today **77**, 419 (2003).
2. M. Haruta, Chem. Rec. **3**, 75 (2003).
3. M. Haruta, T. Kobayashi, H. Sano, N. Yamada, Chem. Lett. **16**, 405 (1987).
4. G. R. Bamwenda, S. Tsubota, T. Nakamura, M. Haruta, Catal. Lett. **44**, 83 (1997).
5. G. C. Bond, D. T. Thompson, Catal. Rev. – Sci. Eng. **41**, 319 (1999).
6. S. D. Lin, M. Bollinger, M. A. Vannice, Catal. Lett. **17**, 245 (1993).
7. S. Tsubota, D. A. H. Cunningham, Y. Bando, M. Haruta, Stud. Surf. Sci. Catal. **91**, 227 (1995).
8. W. S. Epling, G. B. Hoflund, J. F. Weaver, S. Tsubota, M. Haruta, J. Phys. Chem. **100**, 9929 (1996).
9. B. Schumacher, V. Plzak, M. Kinne, R. J. Behm, Catal. Lett. **89**, 109 (2003).
10. S. T. Daniells, M. Makkee, J. A. Moulijn, Catal. Lett. **100**, 39 (2005).
11. T. S. Kim, J. D. Stiehl, C. T. Reeves, R. J. Meyer, C. B. Mullins, J. Am. Chem. Soc. **125**, 2018 (2003).
12. J. D. Stiehl, T. S. Kim, S. M. McClure, C. B. Mullins, J. Am. Chem. Soc. **126**, 13574 (2004).
13. E. E. Stangland, K. B. Stavens, R. P. Andres, W. N. Delgass, J. Catal. **191**, 332 (2000).
14. G. Mul, A. Zwijnenburg, B. van der Linden, M. Makkee, J. A. Moulijn, J. Catal. **201**, 128 (2001).
15. T. Hayashi, K. Tanaka, M. Haruta, J. Catal. **178**, 566 (1998).
16. D. Andreeva, V. Idakiev, T. Tabakova, L. Ilieva, P. Falaras, A. Bourlinos, A. Travlos, Catal. Today **72**, 51 (2002).
17. Q. Fu, H. Saltsburg, M. Flytzani-Stephanopoulos, Science **301**, 935 (2003).
18. Z.-P. Liu, S. J. Jenkins, D. A. King, Phys. Rev. Lett. **94**, 196102. (2005).

19. S. Carrettin, P. McMorn, P. Johnston, K. Griffin, G. J. Hutchings, Chem. Commun. 696 (2002).

20. H. T. Hess in *Kirk-Othmer Encyclopedia of Chemical Engineering*, edited by I. Kroschwitz, M. Howe-Grant (Wiley, New York, 1995).

21. P. Landon, P. J. Collier, A. J. Papworth, C. J. Kiely, G. J. Hutchings, Chem. Commun. 2058 (2002).

22. P. Landon, P. J. Collier, A. F. Carley, D. Chadwick, A. J. Papworth, A. Burrows, C. J. Kiely, G. J. Hutchings, Phys. Chem. Chem. Phys. **5**, 1917 (2003).

23. M. D. Hughes, Y.-J. Xu, P. Jenkins, P. McMorn, P. Landon, D. I. Enache, A. F. Carley, G. A. Attard, G. J. Hutchings, F. King, E. H. Stitt, P. Johnston, K. Griffin, C. J. Kiely, Nature **437**, 1132 (2005).

24. D. C. Meier, X. Lai, D. W. Goodman, in *Surface Chemistry and Catalysis*, edited by A. F. Carley (Kluwer Academic/Plenum Publishers, New York, 2002).

25. M. Valden, S. Pak, X. Lai, D. W. Goodman, Catal. Lett. **56**, 7 (1998).

26. M. M. Schubert, S. Hackenberg, A. C. van Veen, M. Muhler, V. Plzak, R. J. Behm, J. Catal. **197**, 113 (2001).

27. M. A. Bollinger, M. A. Vannice, Appl. Catal. B: Environ. **8**, 417 (1996).

28. J.-D. Grunwaldt, A. Baiker, J. Phys. Chem. B **103**, 1002 (1999).

29. H. M. Ajo, V. A. Bondzie, C. T. Campbell, Catal. Lett. **78**, 359 (2002).

30. Z.-P. Liu, P. Hu, A. Alavi, J. Am. Chem. Soc. **124**, 14770 (2002).

31. G. Mills, M. S. Gordon, H. Metiu, J. Chem. Phys. **118**, 4198 (2003).

32. Y. Xu, M. Mavrikakis, J. Phys. Chem. B **107**, 9298 (2003).

33. H. G. Boyen, G. Kaestle, F. Weigl, B. Koslowski, C. Dietrich, P. Ziemann, J. P. Spatz, S. Riethmueller, C. Hartmann, M. Moeller, G. Schmid, M. G. Garnier, P. Oelhafen, Science **297**, 1533 (2002).

34. N. Lopez, J. K. Nørskov, Surf. Sci. **515**, 175 (2002).

35. N. A. Hodge, C. J. Kiely, R. Whyman, M. R. H. Siddiqui, G. J. Hutchings, Q. A. Pankhurst, F. E. Wagner, R. R. Rajaram, S. E. Golunski, Catal. Today **72**, 133 (2002).

36. M. Date, M. Okumura, S. Tsubota, M. Haruta, Angew. Chem. –Int. Edit. **43**, 2129 (2004).

37. F. Boccuzzi, A. Chiorino, J. Phys. Chem. B **104**, 5414 (2000).

Chapter 2: Cryogenic CO Oxidation on TiO_2 Supported Gold Nanoclusters Pre-covered with Atomic Oxygen

INTRODUCTION

Bulk gold has long been regarded as a "noble" metal, having very low chemical and catalytic activity.[1,2] However, largely through the work of Haruta and coworkers, metal oxide supported gold particles, particularly those that are less than 5 nm in diameter, have been found to have remarkable catalytic properties.[3] In recent years, gold clusters supported on titania (Au/TiO_2) have been shown to be very active catalysts for selective oxidation of propene, nitrogen oxide reduction, and relatively low temperature CO oxidation.[3,4] However, a microscopic understanding of these reactions on Au/TiO_2 has yet to be attained, as the effect of gold particle size and details regarding the reaction mechanism remain unresolved.

In this study we show that impinging gas-phase CO molecules react readily with oxygen adatoms (O_a) pre-adsorbed on $Au/TiO_2(110)$ planar model catalyst to produce CO_2 under ultrahigh vacuum conditions in which the sample is cryogenically cooled. On hydrated Au/TiO_2 powder catalysts prepared by the deposition-precipitation method followed by calcination, Boccuzzi *et al*. have shown that with pre-adsorption of CO on the catalyst the reaction with molecular O_2 will produce CO_2 at 90 K, whereas with molecular oxygen pre-adsorption, the reaction is completely inhibited.[5] In order to focus on the reactivity of oxygen adatoms, and since the dissociation probability of molecular oxygen on our samples is immeasurably low, we expose the surface to an atomic oxygen source to populate the surface with oxygen adatoms. Bondzie *et al*. have

previously shown that CO is oxidized rapidly on the oxygen adatom pre-covered Au/TiO_2 model catalyst surface at room temperature.[6] Here we extend their results to sample temperatures as low as 65 K and also investigate the effects of gold cluster size and oxygen adatom coverage on the CO oxidation reaction.

EXPERIMENTAL

The experiments were conducted in a molecular beam surface scattering apparatus consisting of an ultrahigh vacuum scattering chamber[7] equipped with an Auger electron spectrometer, low energy electron diffraction optics, quadrupole mass spectrometer (QMS), quartz crystal microbalance (QCM), and a custom built metal doser which is used for vapor depositing gold on TiO_2. The $TiO_2(110)$ crystal is mounted on a tantalum plate that can be resistively heated and is in thermal contact with a liquid nitrogen bath. A type K thermocouple is spot-welded to the backside of the tantalum plate to monitor the temperature of the sample.

Gold nanoclusters are deposited on TiO_2 at 300 K by carefully following a procedure published by Lai *et al*.,[8] who have shown via scanning tunneling microscopy that the size of gold nanoclusters grown on TiO_2 can be controlled by varying the amount of vapor-deposited gold. In this study, the quantity of gold deposited, reported in monolayers (ML), is determined by using the QCM. Here, 1 ML of gold refers to a single atomic

layer of close-packed gold (1.387×10^{15} atoms/cm^2), which has a thickness of approximately 2.35 Å. A supersonic beam of oxygen atoms produced from a radio

frequency (RF) generated plasma source[9,10] is directed at the surface in order to pre-adsorb oxygen adatoms. Although we see immeasurable adsorption of molecular oxygen from exposure to an O_2 molecular beam, the RF plasma jet source may generate some excited oxygen molecules, which could have an enhanced molecular adsorption probability. To check that the surface was exclusively pre-covered with oxygen adatoms after exposure to the RF plasma jet source, the sample was heated to 400 K, a temperature well below the associative desorption peak temperature (~600 K, heating rate = 5 K/s) for atomic oxygen on the Au/TiO_2 surface, to induce either dissociation or desorption of any molecularly adsorbed oxygen species: this annealing process did not change the reactivity of the surface. Finally, a continuous molecular beam of pure carbon monoxide (flux ~ 9 x 10^{13} molecules/cm^2-s) is impinged upon the surface immediately after oxygen atom adsorption (without annealing) to study the reaction of CO with oxygen adatoms on the various Au/TiO_2 model surfaces.

RESULTS AND DISCUSSION

Figure 2.1 shows a series of experiments, performed in the manner described above, for gold coverages ranging from 0.25 ML to 30 ML.[11] As shown in Figure 2.1, CO oxidation occurs even at a temperature of 77 K when the carbon monoxide beam impinges on the oxygen pre-covered $Au/TiO_2(110)$ surface. Similar results, not shown here, have been obtained with sample temperatures as low as 65 K. These model catalyst samples were pre-covered with a comparable percentage (50-70 % of saturation coverage) of oxygen adatoms prior to directing the carbon monoxide beam at the

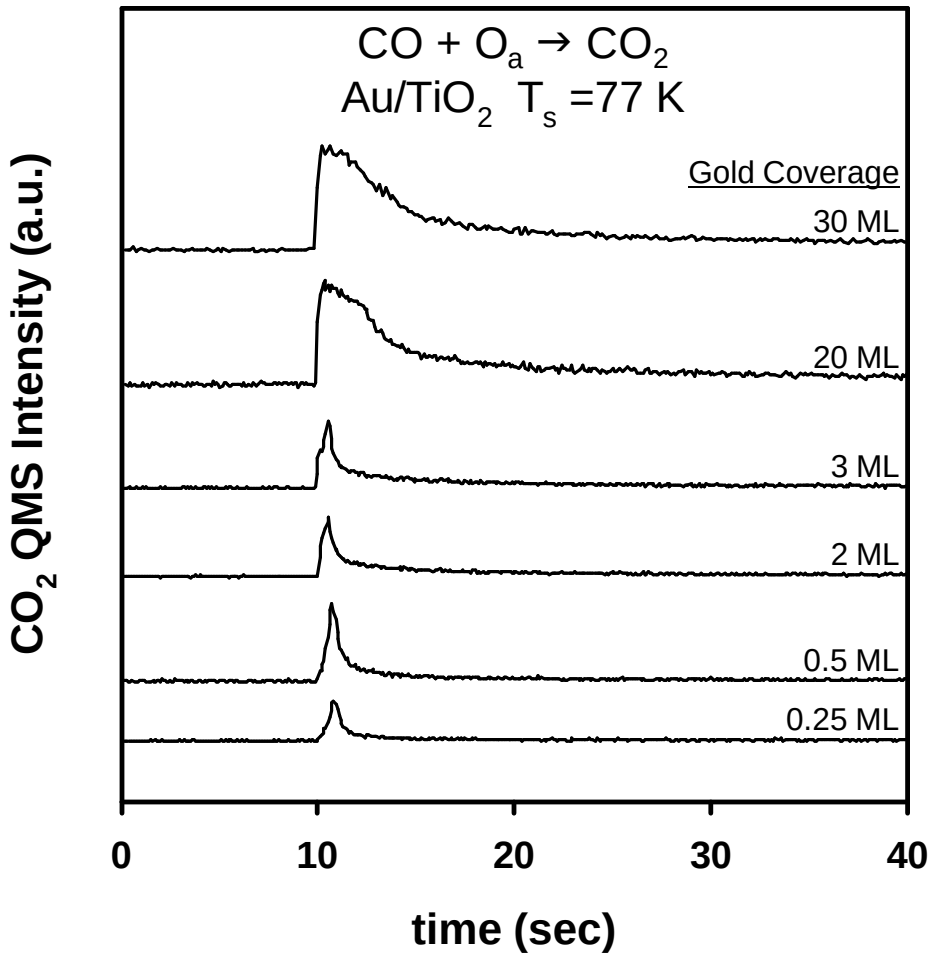

Figure 2.1: Evolution of CO_2 from various amounts of gold on TiO_2 at 77 K. For all samples oxygen atoms were pre-adsorbed prior to impinging a continuous CO beam (starts at t = 10 sec.) on the surface.

Au/TiO_2 surface. Carbon monoxide molecules adsorb on the surface and react with oxygen adatoms to produce CO_2, which then promptly desorbs from the surface. Apparently, atomic oxygen is bound weakly enough on gold such that an adsorbed CO can abstract an O atom with a very small activation barrier.[11] Blank experiments employing an inert flag that can be placed in front of the sample verify that the CO_2 production is directly related to CO impinging on the Au/TiO_2 surface. In our experiments, carbon dioxide is produced only if gold has been deposited on the TiO_2(110) surface and oxygen adatoms are pre-adsorbed on the model catalyst sample.

Although the surfaces with more gold (i.e., 20 and 30 ML) produce more CO_2 as seen from the integrated area of the CO_2 signal, this is likely because most of the surface is covered by gold, hence more oxygen atoms adsorbed on gold are available for reaction with CO. Nevertheless, rapid CO_2 production is clearly seen on all surfaces with different particle sizes, including the surfaces nominally covered by continuous gold films (20 ML, 30 ML). While Valden *et al*., in their studies of CO oxidation employing *molecular oxygen*, report a strong size effect in which a maximum in activity was observed at an average gold particle diameter of 3.5 nm followed by a drastic drop in activity for average particle sizes larger than 6 nm,[12] we see little change in CO_2 production from *atomically adsorbed oxygen* with different particle sizes. As noted by Bondzie *et al*.[6] regarding CO oxidation employing gaseous *molecular oxygen*, our findings support the notion that if reactive oxygen is supplied mainly through dissociation of oxygen molecules on the surface, the rate-limiting step in CO oxidation over gold is likely the dissociation of molecular oxygen and the particle size effect seen by Haruta, Goodman, and coworkers[3,12] may be due to this elementary step.

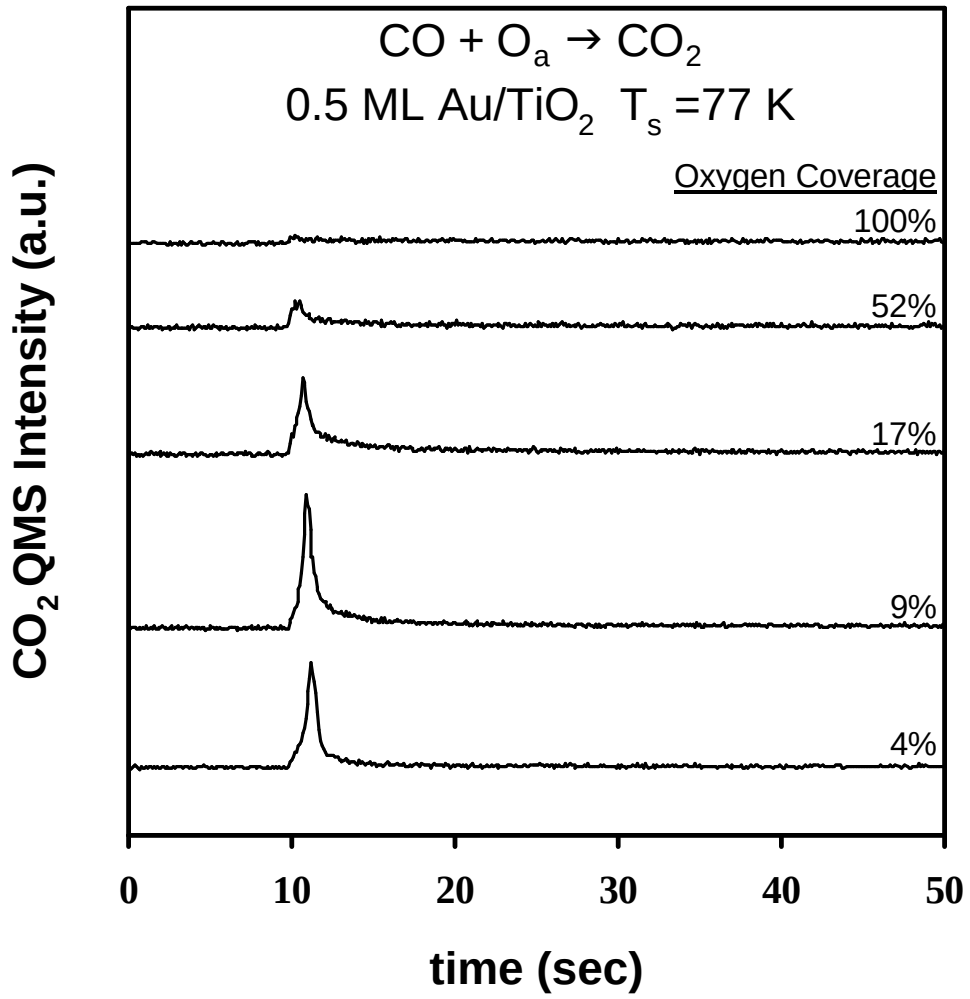

Figure 2.2: Evolution of CO_2 from a 0.5 ML of gold on TiO_2 with different oxygen atom coverages at 77 K. For all samples oxygen atoms were pre-adsorbed prior to impinging a continuous CO beam (starts at t = 10 sec.) on the surface.

Figure 2.2 shows CO_2 production as a function of oxygen coverage with 0.5 ML (~3.1 nm diameter on average)[8] of gold on TiO_2 at 77 K. As more atomic oxygen is pre-adsorbed, above a coverage of ~10% relative to saturation, less CO_2 is produced with a continuous CO beam of the same intensity. The CO uptake by the surface also decreases as the oxygen coverage increases from 4% relative coverage to saturation coverage thus explaining some of the decrease in CO_2 production seen with higher oxygen coverages. It may be that when the oxygen coverage is relatively high, there are fewer sites for CO to adsorb upon thus resulting in less CO_2 production and/or that oxygen adatoms change the electronic properties of the gold particles so that CO adsorption and reaction is hindered.

We note that even though CO_2 production drastically drops after approximately 3-5 seconds of exposure to the CO beam, there is still a considerable amount of oxygen remaining on the sample (as determined from desorption measurements). Also, the reaction probability of an adsorbed CO molecule to convert to carbon dioxide is only on the order of ~5%. Why the remaining oxygen is not reacting more rapidly with adsorbed and/or impinging CO molecules is not currently understood and remains a subject of further investigation.

CONCLUSION

In conclusion, we have shown that CO reacts readily with pre-adsorbed oxygen atoms on a Au/TiO_2 planar model catalyst to produce CO_2 even at temperatures as low as 65 K. Gold particle size seems to have little effect on the CO oxidation reaction when oxygen adatoms are pre-adsorbed. We have also shown that as the oxygen adatom

coverage increases, the rate of CO oxidation decreases on Au/TiO_2 at cryogenic temperatures.

REFERENCES

1. G. C. Bond, D. T. Thompson, Catal. Rev.–Sci. Eng. **41**, 319 (1999).
2. B. Hammer, J. K. Nørskov, Nature **376**, 238 (1995).
3. M. Haruta, Catal. Today **36**, 153 (1997); CATTECH **6**, 102 (2002).
4. G. C. Bond, D. T. Thompson, Gold Bull. **33**, 41 (2000).
5. F. Boccuzzi, A. Chiorino, M. Manzoli, P. Lu, T. Akita, S. Ichikawa, M. Haruta, J. Catal. **202**, 256 (2001).
6. V. A. Bondzie, S. C. Parker, C. T. Campbell, Catal. Lett. **63**, 143 (1999).
7. M. C. Wheeler, D. C. Seets, C. B. Mullins, J. Chem. Phys. **105**, 1572 (1996).
8. X. Lai, T. P. St.Clair, M. Valden, D. W. Goodman, Prog. Surf. Sci. **59**, 25 (1998).
9. J. E. Pollard, Rev. Sci. Instrum. **63**, 1771 (1992).
10. M. C. Wheeler, C. T. Reeves, D. C. Seets, C. B. Mullins, J. Chem. Phys. **108**, 3057 (1998).
11. N. Lopez, J. K. Nørskov, J. Am. Chem. Soc. **124**, 11262 (2002).
12. M. Valden, X. Lai, D. W. Goodman, Science **281**, 1647 (1998).

Chapter 3: Molecular Beam Study of Low Temperature CO Oxidation on Au(111)

INTRODUCTION

Gold, in bulk form, is considered a noble metal because of its resistance to oxidation and corrosion.[1] Thus, heterogeneous catalysts have not typically been composed of gold because of its perceived inertness. However, much recent work has been inspired by the pioneering discovery of the remarkable catalytic activity of oxide-supported gold nanoparticles less than 5 nanometers (nm) in diameter.[2] Indeed, gold nanoparticles supported by various metal oxides such as TiO_2, Al_2O_3, Fe_2O_3, Co_2O_4 etc., have been shown to catalyze the low-temperature oxidation of CO,[2-7] selective oxidation of propene,[8,9] nitrogen oxide reduction,[10] and several other reactions.[11-13] It is not fully understood why gold nanoparticles are catalytically active, but since these seminal findings, additional information has been acquired regarding the ability of bulk gold to catalyze select reactions. Thus, it is useful to contrast and compare the efficacy of reactions over gold in bulk and nanoparticle form in order to better understand gold chemistry.

In a recent study we showed that impinging, gas-phase CO molecules will readily react with oxygen adatoms pre-adsorbed on a TiO_2(110) crystal populated with gold nanoclusters to produce gas-phase CO_2 at sample temperatures as low as 65 K.[14] Further, we observed that gold particle size appeared to have little effect on the reactivity; prompt CO_2 production was even detected on the surface of a relatively thick (30 Layers), continuous gold film (on TiO_2) covered with oxygen adatoms at low

temperature. This result, plus the fact that Au(111) is the most stable configuration of bulk gold and is expected to dominate the gold nanoparticle surface, motivated us to study low temperature CO oxidation on the oxygen atom precovered Au(111) single crystal surface.

Previous studies have shown that CO can be oxidized to CO_2 on gold single crystal surfaces that have been precovered with oxygen atoms. Outka et al. report that CO_2 is produced with negligible activation energy when a Au(110) single crystal, precovered with atomic oxygen, is exposed to CO at 300 K.[15] More recently, Gottfried et al.[16] performed an in depth study of CO oxidation on Au(110) over a broad temperature range. After a known coverage of oxygen adatoms was generated on the surface from electron irradiation of physically adsorbed molecular oxygen, the surface was heated (2.35 K/s) in an ambient of CO (1×10^{-6} mbar). CO_2 desorption peaks were observed at approximately 67 K, 105 K, and 175 K. The low temperature peak at 67 K was attributed to CO_2 having enough energy to surmount the desorption activation barrier after formation. The desorption peak at 105 K was attributed to CO_2 formed on the surface between 67 K and 105 K. In a separate experiment in which CO_2 was adsorbed on an oxygen covered Au(110) surface, Gottfried et al. observed CO_2 to desorb around 105 K, supporting their interpretation. Lastly, the feature at 175 K was ascribed to a balance between the surface reaction rate constant increasing and the steady-state CO surface population decreasing with increasing substrate temperature. Also, Gottfried et al.[17] have shown via ultraviolet photoelectron spectroscopy that CO can be oxidized at sample temperatures as low as 45 K on Au(110). Finally, Koel et al.[18,19] have shown

that CO is oxidized exothermically on Au(111) precovered with atomic oxygen at temperatures between 250 and 375 K.

In this paper we present results of our investigation of the low-temperature oxidation of CO on an oxygen atom precovered Au(111) single crystal. In particular, the effect of oxygen precoverage on the initial reactivity of incident CO molecules is discussed. Further, we show that CO can be oxidized at temperatures as low as 77 K on the oxygen precovered Au (111) surface.

EXPERIMENTAL

The experiments were performed in a molecular beam surface scattering apparatus that has been described previously,[14, 20] but is briefly summarized here. The apparatus consists of an ultrahigh vacuum (UHV) scattering/analysis section and a quadruply differentially-pumped molecular beam source section. The scattering/analysis chamber (base pressure less than 2.0×10^{-10} Torr) is equipped with an Auger electron spectrometer (AES), low energy electron diffraction optics (LEED), quadrupole mass spectrometer (QMS), an ion gun, and an inert flag, which can be inserted in front of the sample to scatter the beam.

The sample consists of a Au(111) single crystal (11mm in diameter, 1.5 mm thick) mounted to a tantalum plate that can be resistively heated and is in thermal contact with a liquid nitrogen bath. Oxygen atoms were deposited on the surface using a radio frequency (RF) generated plasma source that produced a supersonic beam of O atoms from an 8% (vol.) O_2 in Ar gas mixture. The oxygen atom source is a modification of a

design by Pollard.[21-23] An oxygen dissociation fraction of ~40%, as measured by time of flight techniques, is achieved. Ions were deflected from the O-atom beam by a charged plate biased at 3000 V, located below the beam line in one of the differential pumping stages.

Both the oxygen beam and the CO beam were expanded from the same nozzle through the same apertures to ensure that the beam spots on the gold sample were the same in size and coincident. The RF generator was switched on only when it was necessary to dose atomic oxygen through the nozzle. The beam spot (~3 mm in diameter) was much smaller than the sample size to minimize effects from impinging gas interacting with other surfaces in the chamber. A typical value for the CO beam flux was ~9×10^{13} molecules / $cm^2 \cdot$ s. The Au(111) surface was cleaned by argon ion sputtering followed by annealing in UHV to eliminate carbon and other surface impurities. The cleaning cycle was repeated until no appreciable impurity signal could be detected by AES. Surface crystallinity was verified by LEED.

RESULTS AND DISCUSSION

Figure 3.1 shows temperature programmed desorption (TPD) spectra of O_2 from Au(111) for various oxygen atom coverages. Relative oxygen coverages were calculated by integrating the area under the TPD curves. In order to determine the absolute oxygen coverages, Auger electron spectra (AES) were collected for each oxygen atom dose (inset of Figure 3.1). The absolute oxygen coverages were estimated by comparing the O/Au AES ratio to the O/Pt AES ratio. On Pt(111), the O/Pt ratio is 0.3

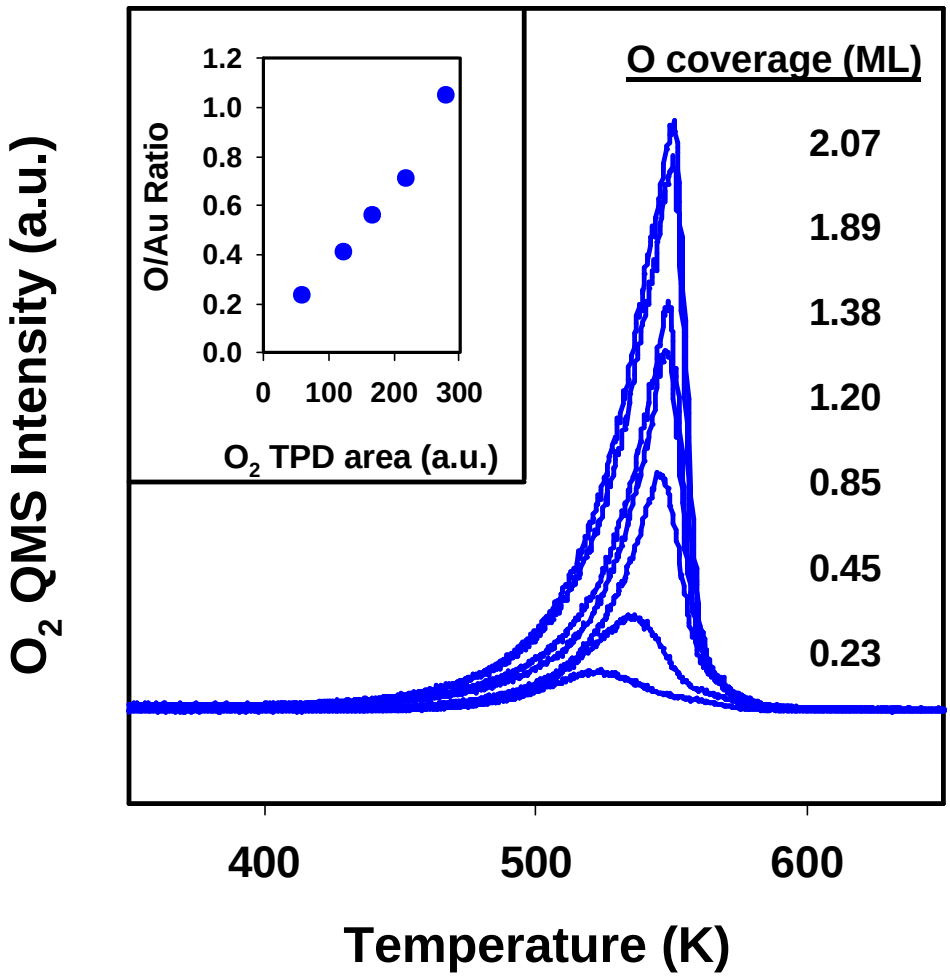

Figure 3.1: O_2 TPD spectra of various oxygen atom coverages on Au(111) (heating rate : β = 3 K/s). Inset shows O/Au AES signal ratio vs. integrated O_2 TPD area for 0.23, 0.45, 0.85, 1.20, 1.38 ML of oxygen covered Au(111).

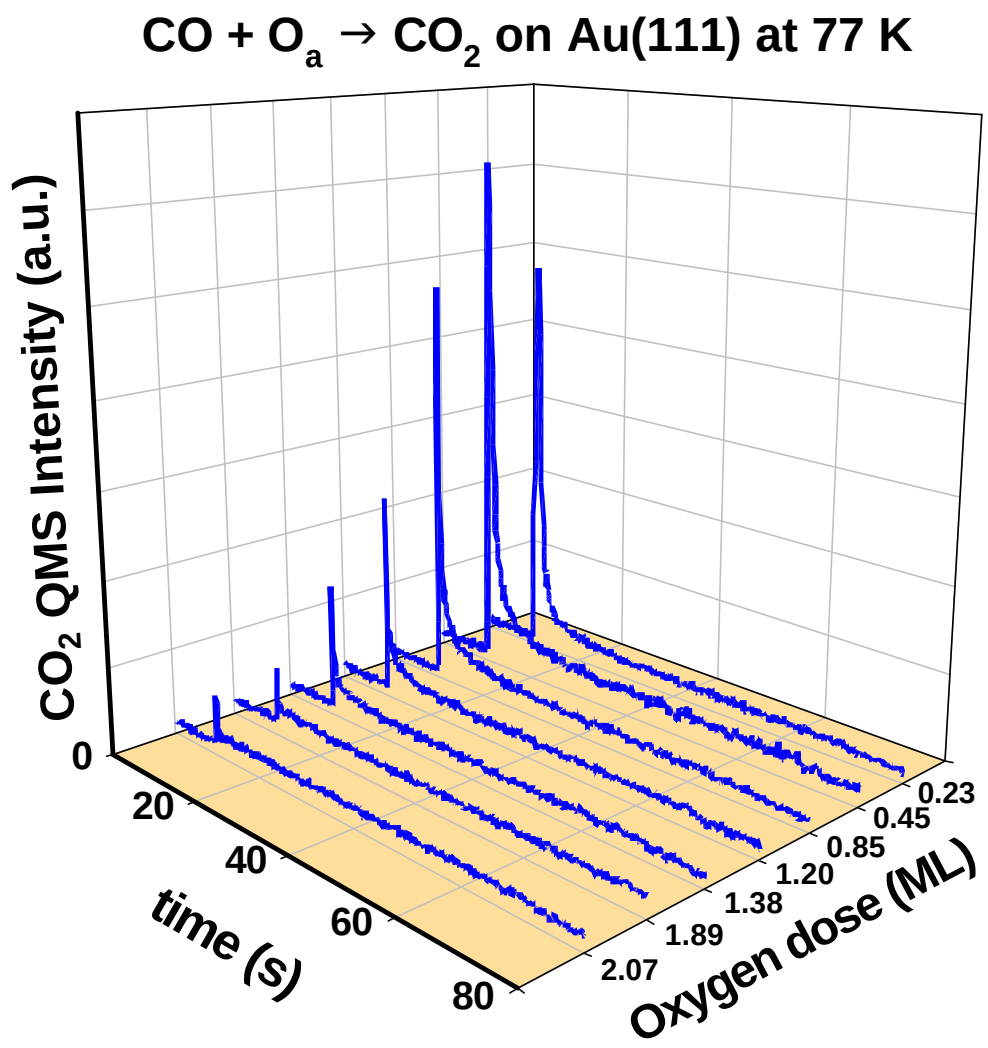

Figure 3.2: CO_2 QMS signal from oxygen covered Au(111) surfaces at 77 K during CO molecular beam impingement. CO beam starts at 10 sec for all oxygen coverages.

for a (2×2) oxygen adlayer composed of 3.93×10^{14} O atoms/cm^2 and a Au to Pt AES ratio of 0.95 was used as a conversion factor.[15] Here, 1ML of oxygen is defined as 1.387×10^{15} atoms/cm^2 and refers to a single atomic layer of close-packed gold. As can be seen in the inset of Figure 3.1, at relatively low oxygen coverages, the O/Au AES ratio increases linearly as the O_2 TPD area increases. Therefore the absolute oxygen coverage on Au(111) can be calculated from the O_2 TPD area by using the calibration curve.

Figure 3.2 shows the CO_2 QMS signals observed while impinging the CO molecular beam on the Au(111) surface with various O coverages (0.23 – 2.07 ML) at 77 K. We have shown that if the RF-generated plasma is used to populate the surface with atomic oxygen, a small amount of molecular oxygen is also present on the surface.[24] Thus, the sample was heated to 300 K to eliminate any molecularly adsorbed oxygen from the surface prior to CO impingement at 77 K. As shown in Figure 3.2, for all oxygen coverages, prompt CO_2 production was observed when the sample was exposed to the CO beam (CO beam exposure began at t = 10 seconds) followed by a sharp decrease in CO_2 production. Despite a lack of detectable CO_2 production at long CO exposure times, TPD measurements show that oxygen atoms still remain on the surface after the CO beam exposure is stopped. At oxygen precoverages greater than ~1.5 ML, the majority of oxygen adatoms do not react with impinging CO molecules on our experimental time scale.

The initial reaction probability of *adsorbed* CO was measured to be ~15%. With all of the oxygen precovered surfaces studied, if the CO beam is impinged on the surface

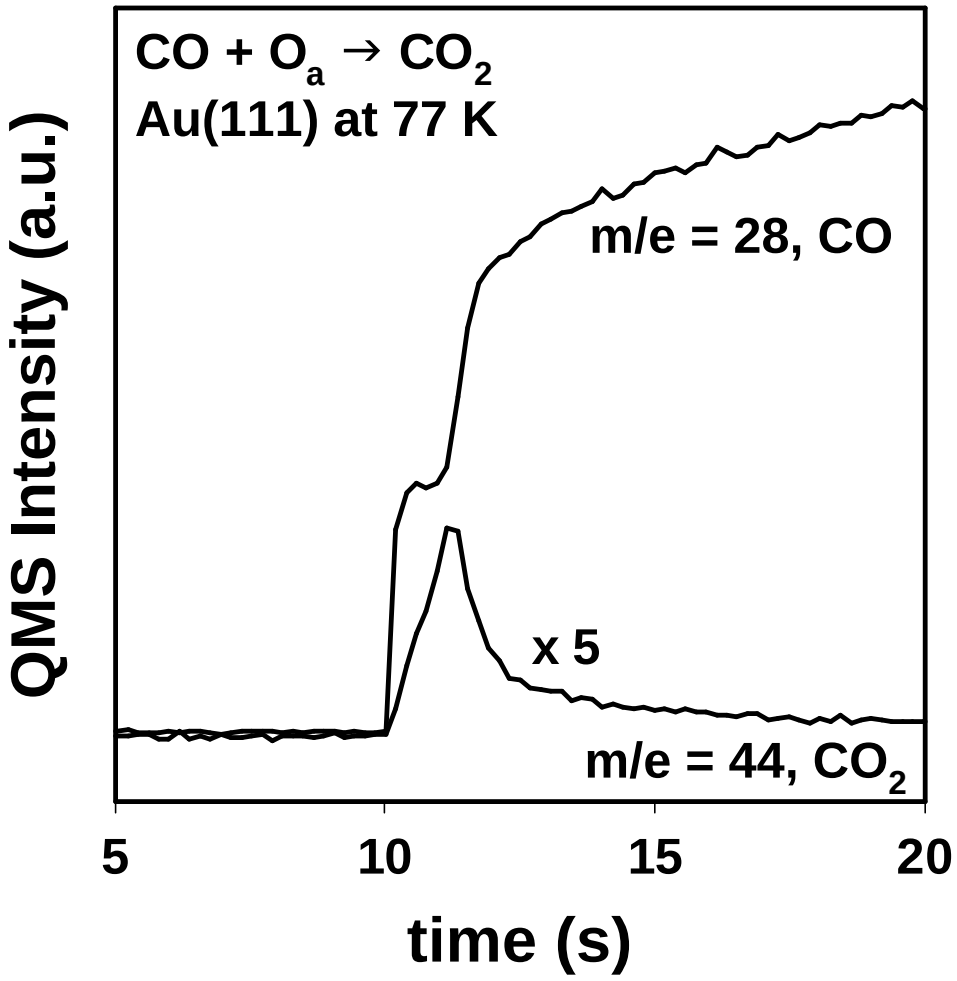

Figure 3.3: CO and CO_2 QMS signal during CO impingement on O covered Au(111) surface at 77 K. The oxygen precoverage was 0.45 ML and the CO beam starts at 10 sec.

immediately after the oxygen dose, i.e., prior to heating the sample to 300 K, the initial CO_2 production is always higher than that of the annealed surface with the same oxygen precoverage. Gottfried et al.[17] have also reported similar phenomena and they speculate that the annealing process can lead to formation of oxygen adatom islands, which are less reactive with CO.

As can be seen from the CO_2 QMS intensities shown in Figure 3.2, there is strong coverage dependence on CO oxidation at 77 K. At oxygen precoverages up to 0.5ML, CO_2 production increases with oxygen precoverage because of the additional availability of oxygen. At oxygen precoverages above 0.5ML, the initial CO_2 production (based on integrated peak area) decreases with increasing oxygen precoverage. This appears to occur because the adsorbed oxygen atoms begin to inhibit CO adsorption on the surface and limit the reaction rate. Adsorbed O atoms can modify the electronic and geometric structures of the Au(111) surface. Saliba et al. have shown that 1.0 ML of oxygen on Au(111) increases the work function by 0.80 eV.[25] So the decrease in CO uptake with increasing oxygen coverage could result from the changes in the electronic structure of the surface and/or from adsorption site blocking by oxygen adatoms.

Another interesting feature observed is that the CO_2 production peak seems to coincide with the onset of CO saturation on the surface. Figure 3.3 shows CO uptake and CO_2 production on Au(111) with 0.45 ML of oxygen adatoms. It should be noted that the amount of CO detected is due to reflection of CO from the surface and the amount of CO_2 observed is a result of adsorbed CO and oxygen adatom reacting with each other. Thus, the abrupt rise in the CO signal seen here(~12s) corresponds to the accumulation of CO on the oxygen covered Au(111) surface at 77 K. It can be seen that

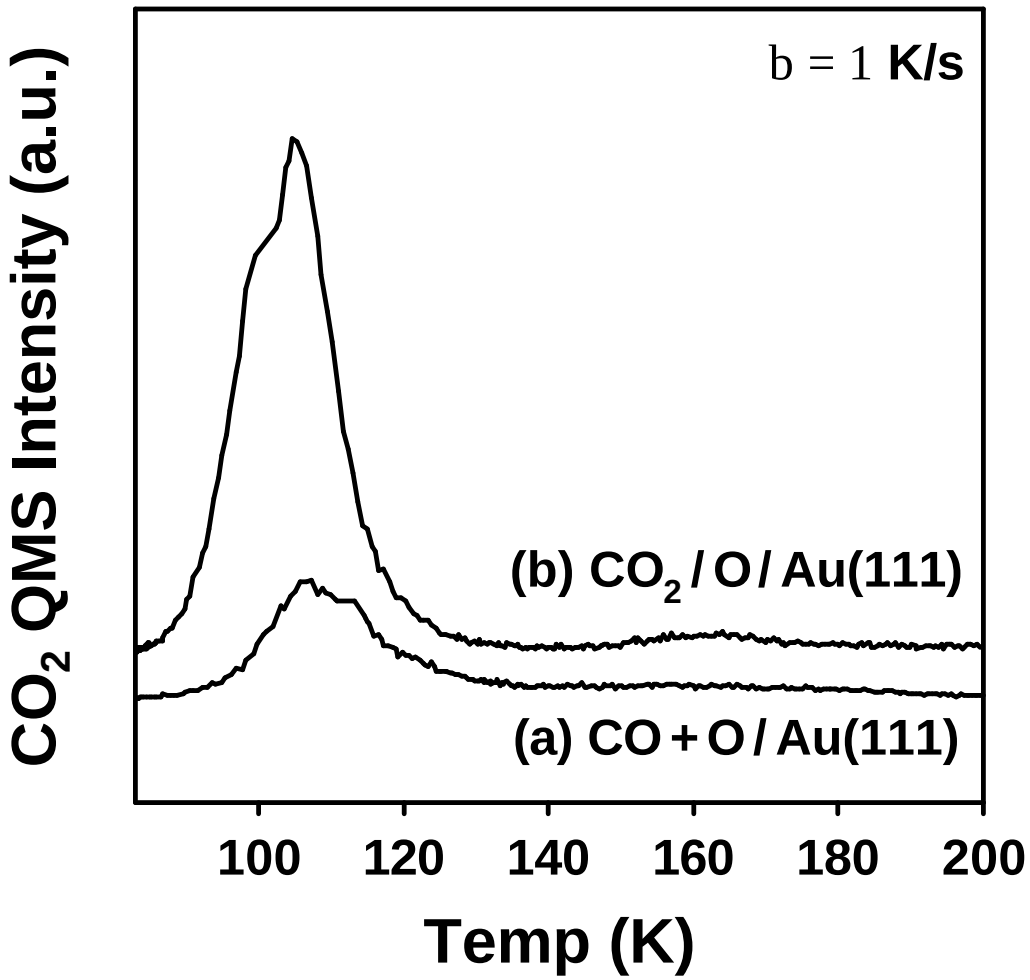

Figure 3.4: CO_2 TPD measurement after (a) CO dose on O covered Au(111) at 77 K, (b) CO_2 dose on O covered Au(111) at 77 K. The O/Au(111) surface was given a saturation dose of CO_2 before performing TPD.

as the sample starts to saturate with CO, CO_2 production starts to decay rapidly. If a TPD is performed after CO exposure, unreacted CO is seen to desorb around ~108 K, which suggests that considerable amount of CO is adsorbed on the oxygen covered gold without reacting with the remaining oxygen on the surface. It seems that once the surface is saturated with CO at 77 K, the reaction shuts off although there are plenty of reactants on the surface. CO oxidation with other oxygen precoverages showed similar behavior, indicating that CO_2 production at 77 K is largely limited by CO uptake on the sample.

Figure 3.4(a) shows a TPD of CO_2 following CO impingement on 0.85 ML of oxygen covered Au(111). As can be seen from the TPD spectrum in Figure 3.4(a), the peak desorption temperature of CO_2 is approximately 108 K (heating rate : ß = 1.0 K/s). The origin of this CO_2 is thought to be the reaction product between adsorbed, unreacted CO and oxygen adatoms on the surface during the heating of the sample. The amount of CO desorption is much greater than CO_2 created during the heating (not shown here), demonstrating that CO signal is not just from the fragmentation of CO_2. Thus, it is likely that this is from CO_2 that is formed via a Langmuir-Hinshelwood mechanism during the heating ramp and not due to CO_2 formed during CO impingement. On platinum, nascent CO_2 is formed on the repulsive wall of the surface interaction potential. This is due to the fact that in CO chemisorption the molecule and oxygen adatom are deeper into the surface compared to the physisorbed CO_2 on Pt(111). Consequently, the nascent CO_2 will have a high translational energy during desorption.[26, 27] A similar argument can be made for CO oxidation on Au(111) and thus we would expect CO_2 made at 77 K during CO impingement to desorb promptly upon formation, leaving a negligible amount of CO_2 on the surface. However, we cannot be rule out that this

desorption feature may be due to CO_2 formed during the CO exposure at 77 K and remaining on the surface with subsequent desorption at ~108 K during the TPD. When CO_2 is adsorbed on an oxygen covered Au(111) surface (CO_2 does not populate our clean Au(111) surface), a desorption feature peaked at ~108 K is observed (Figure 3.4(b)).

We note in passing that CO_2 can also be produced by directing high kinetic energy (~1 eV) Kr beam, which is generated by seeding 2 % Kr in He, at the surface with CO and oxygen atoms coadsorbed on Au(111) at 77 K. As in the TPD measurement, lot more CO is observed than CO_2. Details of this collision induced reaction procedures are published elsewhere.[28]

The reaction occurring at 77 K when CO is impinged on a O-precovered surface may follow a slightly different mechanism than the classical Langmuir-Hinshelwood mechanism. A classical Eley-Rideal (E-R) mechanism can probably be excluded as the dominant mechanism since we observe the CO_2 production to be a strong function of sample temperature (not shown here) and the initial reactivity in an E-R mechanism should be fairly independent of the surface temperature since the gas phase species is pictured to react directly with the adsorbed moieties.

We can hypothesize that the prompt reaction at 77 K that we observe is proceeding through a precursor-mediated reaction mechanism,[29] which can be thought of as a special case of the Langmuir-Hinshelwood mechanism. In the precursor-mediated reaction mechanism we are suggesting, the CO is in a physically adsorbed, trapped (precursor) state instead of a chemisorbed state. However, the oxygen atom is in a chemisorbed state. Based on the results in Figure 3.2, it appears that once a CO molecule

falls into the chemisorbed state, it does not readily react with adjacent O atoms, and likely blocks other impinging CO molecules from reacting with oxygen adatoms.

In a classical Langmuir-Hinshelwood mechanism, even though the reaction occurs between chemisorbed species, at some point, the chemisorbed species must be activated and somewhat mobile in order to react with the other reactant on the surface. This activated reactant can be thought of as being in a precursor state having high mobility on the surface, which can readily react with other adsorbates on the surface once encountered. Thus, there is not a clear distinction between the two reaction mechanisms. However, for our system at 77 K, it appears that once the precursor on the surface falls into the chemisorbed CO state, there is not sufficient thermal energy to activate the chemisorbed CO back into the precursor state thus allowing for a distinction between the classical Langmuir-Hinshelwood mechanism and the precursor-mediated mechanism. In addition, the Langmuir-Hinshelwood mechanism seems to come into play at higher temperatures, because we see CO_2 production between the remaining adsorbed CO and O when we heat the sample.

CONCLUSION

CO oxidation on oxygen precovered Au(111) was measured using molecular beam techniques at a sample temperature of 77 K as a function of oxygen coverage. Prompt CO_2 production was seen when the CO beam impinges on the sample followed by an exponential decay of CO_2 production in all cases. At oxygen precoverages above 0.5 ML, the initial CO_2 production decreases with increasing oxygen precoverage mainly

due to the decrease in CO uptake with increasing O precoverage. CO oxidation at 77 K is believed to be going through a precursor mediated reaction mechanism, where CO is in a precursor state or trapped state and oxygen atoms are in a chemisorbed state.

REFERENCES

1. G. C. Bond, D. T. Thompson, Catal. Rev. –Sci. Eng. **41**, 319 (1999).

2. M. Haruta, N. Yamada, T. Kobayashi, and S. Iijima, J. Catal. **115**, 301 (1989).

3. M. Haruta, S. Tsubota, T. Kobayashi, H. Kageyama, M. J. Genet, and B. Delmon, J. Catal. **144**, 175 (1993).

4. M. Okumura, S. Nakamura, S. Tsubota, T. Nakamura, M. Azuma, and M. Haruta, Catal. Lett. **51**, 53 (1998).

5. J.-D. Grunwaldt, M. Maciejewski, O.S. Becker, P. Fabrizioli, A. Baiker, J. Catal. **186**, 458 (1999).

6. F. Boccuzzi, A. Chiorino, J. Phys. Chem. B **104**, 5414 (2000).

7. B. Schumacher, V. Plzak, M. Kinne, R. J. Behm, Catal. Lett. **89**, 109 (2003).

8. T. Hayashi, K. Tanaka, M. Haruta, J. Catal. **178**, 566 (1998).

9. B. S. Uphade, T. Akita, T. Nakamura, M. Haruta, J. Catal. **209**, 331 (2002).

10. A. Ueda, M. Haruta, Gold Bulletin **32**, 3 (1999).

11. M. Haruta, Catal. Today **36**, 153 (1997).

12. M. Haruta, CATTECH **6**, 102 (2002).

13. R. Meyer, C. Lemire, Sh. K. Shaikhutdinov, H.-J. Freund, Gold Bulletin **37**, 72 (2004)**.**

14. T. S. Kim, J. D. Stiehl, C. T. Reeves, R. J. Meyer, C. B. Mullins, J. Am. Chem. Soc. **125**, 2018 (2003).

15. D. A. Outka, R. J. Madix, Surf. Sci. **179**, 351 (1987), and references therein.

16. J. M. Gottfried, K. J. Schmidt, S. L. M. Schroeder, K. Christmann, Surf. Sci. **525**, 197 (2003).

17. J. M. Gottfried, Ph. D. thesis, the Freie Universität Berlin (2003)

18. M. A. Lazaga, D. T. Wickham, D. H. Parker, G. N. Kastanas, B. E. Koel, ACS Sym. Ser. **523**, 90 (1993).

19. D. H. Parker, B. E. Koel, J. Vac. Sci. Technol. A **8**, 2585 (1990).

20. M. C. Wheeler, D. C. Seets, C. B. Mullins, J. Chem. Phys. **105**, 1572 (1996).

21. J. E. Pollard, Rev. Sci. Instrum. **63**, 1771 (1992).

22. M. C. Wheeler, D. C. Seets, C. B. Mullins, J. Chem. Phys. **107**, 1672 (1997).

23. M. C. Wheeler, C. T. Reeves, D. C. Seets, C. B. Mullins, J. Chem. Phys. **108**, 3057 (1998).

24. J. D. Stiehl, T. S. Kim, S. M. McClure, C. B. Mullins, J. Am. Chem. Soc. **126**, 1606 (2003).

25. N. Saliba, D. H. Parker, B. E. Koel, Surf. Sci. **410**, 270 (1998).

26. C. A. Becker, J. P. Cowin, L. Wharton, D. J. Auerbach, J. Chem. Phys. **67**, 3394 (1977).

27. C. B. Mullins, C. T. Rettner, D. J. Auerbach, J. Chem. Phys. **95**, 8649 (1991).

28. J. D. Stiehl, T. S. Kim, C. T. Reeves, R. J. Meyer, C. B. Mullins, J. Phys. Chem. B **108**, 7917 (2004).

29. J. Harris, B. Kasemo, Surf. Sci. **105**, L281 (1981).

Chapter 4: Water Activated by Atomic Oxygen on Au(111) to Oxidize CO at Low Temperatures

INTRODUCTION

Since Haruta's discovery of the exceptional reactivity of gold nanoclusters nearly 20 years ago,[1] there has been an exponential growth in the study of catalytic chemistry on metal oxide supported small gold particles including low temperature CO oxidation,[2-8] direct propylene epoxidation,[9-11] and the water gas shift reaction.[12-14] Although 2-5 nm diameter gold nanoparticles exhibit interesting and important catalytic reactivity in many heterogeneous chemical reactions, oftentimes, details regarding the reaction mechanism remain uncertain. Notably, catalytic CO oxidation over gold clusters require the presence of water to proceed at appreciable rates, where the reaction was reported to be more than 10 times higher with the addition of water in the feed stream.[15,16] It has been postulated that water may assist in either activating the molecular oxygen or, decomposing carbonates formed on the surface.[16,17] Both hypotheses suggest that water is not directly involved, but rather only indirectly promotes the reaction.

Here we show that a Au(111) surface populated with atomic oxygen [^{16}O] and oxygen labeled water [$H_2{}^{18}O$] produces both $C^{16}O^{16}O$ and $C^{16}O^{18}O$ while impinging $C^{16}O$ at low surface temperatures, indicating the direct involvement of water in CO oxidation with OH as a possible reaction intermediate.

The reaction of CO and OH leading to CO_2 formation is widely studied in gas phase chemistry due to the pivotal role of OH radicals in atmospheric chemistry.[18,19] There are also several investigations of CO and OH reaction on metal surfaces,[20-22]

primarily related to electrochemistry. In an ultrahigh vacuum (UHV) study, Bergeld et al. showed that water can promote CO oxidation on oxygen covered Pt(111). They showed that when water is coadsorbed prior to temperature programmed reaction of Pt(111) surface populated with CO and oxygen, a previously unobserved CO_2 desorption peak near 200 K appears. This new peak has been attributed to CO reacting with OH groups on the surface.[22] It is possible that a similar reaction can occur on Au(111) where hydroxyls formed from water splitting are reacting with CO to form CO_2 at low surface temperatures.

EXPERIMENTAL

The experiments were performed in a molecular beam surface scattering chamber that has been described elsewhere,[7,23] but is briefly summarized here. The apparatus consists of a UHV scattering/analysis section and a quadruply differentially-pumped molecular beam source section. The sample consists of a Au(111) single crystal (11mm in diameter, 1.5 mm thick) mounted to a tantalum plate that can be resistively heated and is in thermal contact with a liquid nitrogen bath, while the temperature of the surface is monitored with a type K thermocouple. Oxygen atoms were deposited on the surface using a radio frequency (RF) generated plasma source that produced a supersonic beam of ^{16}O atoms from an 8% (vol.) $^{16}O_2$ in Ar gas mixture. All three beams (oxygen, water, and CO) were expanded from the same nozzle through the same apertures to ensure that the beam spots on the gold sample were the same in size and coincident. The beam spot (~3 mm in diameter) was much smaller than the sample size to minimize effects from

impinging gas interacting with other surfaces in the chamber. The Au(111) surface was cleaned employing standard methods,[7,23] until no appreciable impurity could be detected by auger electron spectroscopy.

RESULTS AND DISCUSSION

Figure 4.1 demonstrates how CO can react with water when oxygen adatoms are present to activate the water on Au(111) at 77 K. In Figure 4.1 (a), a beam of CO is impinged on a 0.18 ML (1 ML = 1.387×10^{15} (atoms or molecules)/cm^2) atomic oxygen covered surface. As can be seen, only mass 44 $C^{16}O^{16}O$ is observed during the CO impingement. In Figure 4.1 (b), the CO beam is impinged on Au(111) with 0.1 ML of isotopically labeled $H_2{}^{18}O$. Without preadsorbed oxygen, CO_2 is not formed on the surface. In Figure 4.1 (c), 0.1 ML of $H_2{}^{18}O$ is dosed over 0.18 ML of atomic oxygen on Au(111), followed by exposure to a CO beam. As can be seen from the data of Figure 4.1 (c), in addition to mass 44 $C^{16}O^{16}O$, a small amount(27 % of total CO_2 production) of mass 46 $C^{16}O^{18}O$ is observed, indicating that oxygen originating from water is directly involved in CO oxidation at 77K on Au(111) when atomic oxygen is preadsorbed on the surface. Another notable feature in this quadrupole mass spectrometer (QMS) spectrum regards the rapid CO_2 signal decay, although there is still a considerable amount of surface oxygen remaining on the surface based on the temperature programmed desorption (TPD) afterwards. This is due to unreacted CO covering the surface, which is also verified from TPD, limiting further reaction.

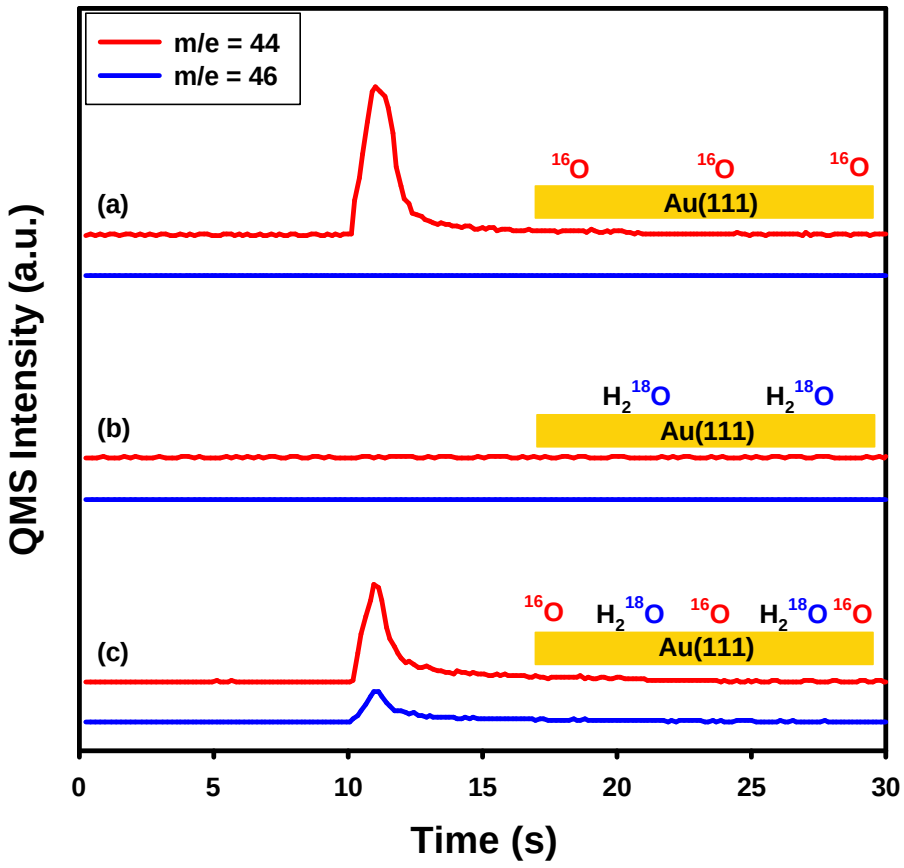

Figure 4.1: Evolution of CO_2 at 77 K while impinging a continuous CO beam (from 10 to 20 sec.) at the surface. The red curve represents mass 44 $C^{16}O^{16}O$ and the blue curve represents mass 46 $C^{16}O^{18}O$ with (a) 0.18 ML of ^{16}O atoms preadsorbed, (b) 0.1 ML of $H_2{}^{18}O$ preadsorbed, and (c) 0.1 ML of $H_2{}^{18}O$ in addition to 0.18 ML of ^{16}O atoms preadsorbed on Au(111) at 77 K. We note that all the procedure was done while the surface temperature was kept at 77 K.

In order to further explore the details of this reaction, we compare the total amount of CO_2 produced from our Au(111) surface solely covered by oxygen with that of the surface covered with both atomic oxygen and water. As mentioned earlier, not all surface oxygen is consumed when a CO beam is impinged on the surface at 77 K. In order to avoid accumulation of CO on the surface, we ran the reaction at Ts = 140K, a temperature well below the desorption peak temperature (175 K) of water on oxygen covered Au(111) but above the desorption peak temperature (108 K) for CO (in order to avoid limiting the extent of reaction).

In Figure 4.2 (a), a CO beam is impinged on a 0.08 ML of oxygen covered surface at 140 K. The area underneath the curve between 10 and 40 seconds represents the amount of mass 44 CO_2 produced as shown in the inset. No mass 46 CO_2 is detected in this case. In Figure 4.2 (b), a CO beam is impinged on a surface where 0.08 ML of oxygen is initially dosed followed by the addition of 0.1 ML of $H_2{}^{18}O$. The red curve represents the amount of mass 44 CO_2 production and the blue curve represents the amount of mass 46 CO_2 [i.e., $C^{16}O^{18}O$] produced during CO impingement. The inset shows the total amount of CO_2 produced for each case in a bar chart, with the red bar representing mass 44 CO_2 and blue bar representing mass 46 $C^{16}O^{18}O$. As shown, with the same amount of preadsorbed ^{16}O on the surface, 77 % more CO_2 production is observed with water added to the surface, similar to what Bergeld et al. have seen on Pt(111).[22] Based on subsequent TPD measurements (not shown), there was no detectable atomic oxygen left on the surface after the CO impingement at 140K. However a small amount (~0.03 ML) of $H_2{}^{18}O$ and $H_2{}^{16}O$ (produced from oxygen scrambling between ^{16}O and $H_2{}^{18}O$) was observed that was not consumed during the reaction. Once the oxygen atoms that activated water to take part in the reaction is completely consumed either by directly reacting with CO or reacting with CO as

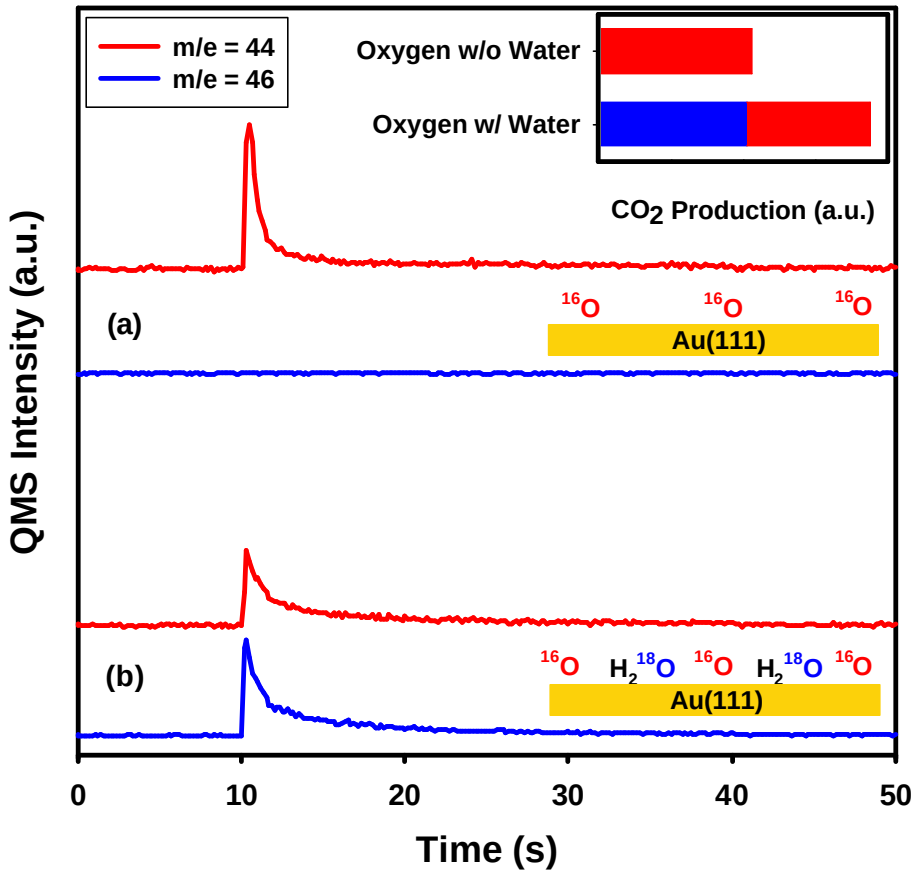

Figure 4.2: Evolution of CO_2 at 140 K while impinging a continuous CO beam (from 10 to 40 sec.) at the surface. Red curve represents mass 44 $C^{16}O^{16}O$ and blue curve represents mass 46 $C^{16}O^{18}O$ with (a) 0.08 ML of ^{16}O preadsorbed, (b) 0.1 ML $H_2{}^{18}O$ in addition to 0.08 ML of ^{16}O atoms preadsorbed on Au(111) at 77 K.

hydroxyls, remaining water on the surface does not seem to react with CO. This is in agreement with the results shown in Figure 4.1 (b) in which adsorbed water alone cannot oxidize CO.

From these results we speculate that OH groups, formed from water interacting with atomic oxygen on Au(111), can participate in oxidizing CO to produce CO_2 on the surface. We have shown that oxygen from adsorbed water will scramble with preadsorbed oxygen atoms on Au(111) and that it is very likely that some water will form hydroxyl on the surface during this oxygen scrambling.[24] And this hydroxyl may be responsible for the mass 46 $C^{16}O^{18}O$ observed. If the mass 46 CO_2 was solely from CO reacting with atomic oxygen (resulting from disproportionation of OH), we would expect to see an equal amount of CO_2 production compared to the surface reaction without water since there would still be approximately the same amount of atomic oxygen on the surface (even if hydrogen atoms from water molecules moved from ^{18}O to ^{16}O). But we clearly see an increase in the total amount of CO_2 produced, indicating that water is activated by atomic oxygen on the surface to take part in the CO oxidation at surface temperatures as low as 77 K. We note that although we tried to account for hydrogen from the reaction, we have yet to detect hydrogen or hydrogen containing species(other than water) during the CO impingement or TPD afterwards.

CONCLUSION

In conclusion, we observe involvement of water in oxidizing impinging CO on oxygen atom precovered Au(111) at low temperatures. CO_2 production was greatly increased with the addition of water on the same oxygen precoverage, and we interpret

these results as due to CO reacting directly with activated water or OH groups formed from water interacting with atomic oxygen on Au(111).

REFERENCES

1. M. Haruta, T. Kobayashi, H. Sano, N. Yamada, Chem. Lett. **16**, 405 (1987).

2. S. D. Lin, M. Bollinger, M. A. Vannice, Catal. Lett. **17**, 245 (1993).

3. S. Tsubota, D. A. H. Cunningham, Y. Bando, M. Haruta, Stud. Surf. Sci. Catal. **91**, 227 (1995).

4. W. S. Epling, G. B. Hoflund, J. F. Weaver, S. Tsubota, M. Haruta, J. Phys. Chem. **100**, 9929 (1996).

5. B. Schumacher, V. Plzak, M. Kinne, R. J. Behm, Catal. Lett. **89**, 109 (2003).

6. S. T. Daniells, M. Makkee, J. A. Moulijn, Catal. Lett. **100**, 39 (2005).

7. T. S. Kim, J. D. Stiehl, C. T. Reeves, R. J. Meyer, C. B. Mullins, J. Am. Chem. Soc. **125**, 2018 (2003).

8. J. D. Stiehl, T. S. Kim, S. M. McClure, C. B. Mullins, J. Am. Chem. Soc. **126**, 13574 (2004).

9. E. E. Stangland, K. B. Stavens, R. P. Andres, W. N. Delgass, J. Catal. **191**, 332 (2000).

10. T. Hayashi, K. Tanaka, M. Haruta, J. Catal. **178**, 566 (1998).

11. G. Mul, A. Zwijnenburg, B. van der Linden, M. Makkee, J. A. Moulijn, J. Catal. **201**, 128 (2001).

12. Z.-P. Liu, S. J. Jenkins, D. A. King, Phys. Rev. Lett. **94**, 196102. (2005).

13. D. Andreeva, V. Idakiev, T. Tabakova, L. Ilieva, P. Falaras, A. Bourlinos, A. Travlos, Catal. Today **72**, 51 (2002).

14. Q. Fu, H. Saltsburg, M. Flytzani-Stephanopoulos, Science **301**, 935 (2003).

15. M. Date, M. Haruta, J. Catal. **201**, 221 (2001).

16. M. Date, M. Okumura, S. Tsubota, M. Haruta, Angew. Chem. –Int. Edit. **43**, 2129 (2004).

17. F. Boccuzzi, A. Chiorino, J. Phys. Chem. B **104**, 5414 (2000).

18. M. I. Lester, B. V. Pond, D. T. Anderson, L. B. Harding, A. F. Wagner, J. Chem. Phys. **113**, 9889 (2000).

19. T. Rockmann, C. A. M. Brenninkmeijer, G. Sauerssig, P. Bergamaschi, J. N. Crowley, H. Fischer, P. J. Cruutzen, Science **281**, 544 (1998).

20. B. E. Hayden, M. E. Rendall, O. South, J. Am. Chem. Soc. **125**, 7738 (2003).

21. T. Lei, M. S. Zei, G. Ertl, Surf. Sci. **581**, 142 (2005).

22. J. Bergeld, B. Kasemo, D. V. Chakarov, Surf. Sci. **495**, L815 (2001).

23. M. C. Wheeler, D. C. Seets, C. B. Mullins, J. Chem. Phys. **105**, 1572 (1996).

24. T. S. Kim, J. Gong, R. A. Ojifinni, J. M. White, C. B. Mullins, Manuscript in Preparation.

Chapter 5: Water Activation by Atomic Oxygen on Au(111) and Reaction of Activated Water with CO at Low Temperatures

INTRODUCTION

Gold is considered as noble among other metals because of its resistance to oxidation and corrosion. It is the most electronegative metal and its electron affinity is actually greater than that of oxygen.[1] For this reason gold will not react directly with other electronegative elements such as molecular oxygen. Although there are cases in which gold has been found to have catalytic properties for some reactions, it is well known for being catalytically inert. As a result, gold has not been given much attention as a potential active ingredient for heterogeneous catalysis until Haruta's discovery of the exceptional reactivity of nanometer sized gold particles nearly 20 years ago.[2] Since the significant findings of Haruta, there has been an exponential growth in gold catalysis research. Some of the reactions studied include low temperature CO oxidation,[3-9] propylene epoxidation,[10-12] and the water gas shift reaction.[13-15] Among these reactions, low temperature CO oxidation is one of the most unique regarding gold catalysts in that it cannot be matched by other metals. This low temperature reactivity has generated great interest and much research of metal oxide supported gold nanoparticles. Although it is widely accepted that gold particles which are 2-5 nm in diameter exhibit the greatest reactivity, there is still much debate on the nature of the active sites for these catalysts and also the details of the reaction mechanism. While some suggest the perimeter interface of gold particles with the metal oxide support as the active site for CO oxidation,[16-19] others point to low coordination sites on small gold particles based on

calculations and gas phase cluster experiments.[20-22] Another issue that is still under debate is the oxidation state of the active form of gold. Some studies state that metallic gold[23,24] is the active form of gold while others claim oxidic gold[25,26] is responsible for the reactivity of gold.

As might be clear from these issues, there are still many questions that need to be resolved in highly active CO oxidation on gold catalysts and further research is necessary to clarify these matters.

Just as CO oxidation is considered to be a classic reaction of choice among many other reactions on metal surfaces, water has enjoyed much attention from the surface science community due to its role in many different surface and interfacial systems. Interaction of water with many different single crystal metal surfaces has been reported and a number of those systems have been shown to irreversibly dissociate water.[27-32]

Another popular system involving water is the coadsorption of water and oxygen on metal surfaces. Water and oxygen coadsorption systems can be divided into mainly two categories: one where water does not dissociate in presence of oxygen on the surface and the other, where oxygen induces water dissociation.

Most metals are known to demonstrate water dissociation with oxygen on the surface. It is commonly believed that oxygen will abstract a hydrogen atom from an adsorbed water molecule to form two OH groups.[33-37] And in some studies, stable water-oxygen complex is observed to be present before forming OH groups.[38-41] In most cases, these OH groups on noble metals have been shown to decompose upon heating to form water and leave an oxygen atom on the surface. On the other hand, unless water can

dissociate on clean metal surfaces on its own, these OH groups that have formed from water-oxygen interaction do not dissociate further to adsorbed hydrogen and oxygen.[42]

While there are many examples that demonstrate oxygen induced water dissociation on metal surfaces, there are only a few cases, which includes Ni(111) and Ru(0001), where water dissociation does not occur on metals with oxygen on the surface.[43-48] These studies commonly observed stabilization of molecular water by preadsorbed oxygen accompanied by desorption temperature shift of water, but did not observe any reaction or even isotopic scrambling between water and oxygen atoms on the surface. Previously, Au(111) was also regarded as a surface where water does not dissociate with oxygen on the surface and like the other metals mentioned above that does not display oxygen induced water dissociation, water is considered to desorb from the oxygen covered surface without reaction, and leave an original oxygen on the surface.[49]

Here, we show that when our radio frequency (RF) generated plasma source is used to generate and deposit oxygen atoms, water interacts with oxygen atoms on the Au(111) surface resulting in oxygen scrambling on the surface. We will also address the role of reactive oxygen state present in our experiments that accounts for previously unobserved reactivity of water on oxygen covered Au(111). There had been several studies claiming the existence of different types of oxygen atoms on the surface in terms of reactivity towards water.[50-54] These studies state that O^{d-} species, which are typically seen at low surface temperatures, are more reactive than O^{2-} species and we will demonstrate the vital role of these reactive oxygen species (which will be referred to as metastable oxygen in this paper) in surface reactions on Au(111).

Going back to CO oxidation on gold catalysts, another notable aspect of low temperature CO oxidation is that the addition of water in the feed stream is believed to enhance the reactivity by as much as two orders of magnitude.[55] It has been postulated that water can promote the reaction by either activating the molecular oxygen on the surface to enhance CO_2 production or help decompose the carbonates that may accumulate on the surface to accommodate additional reactants to react on the surface. These hypotheses both propose that water is not directly participating in the reaction, but only indirectly assisting the reaction.

Here we show unambiguous evidence of how water can participate in CO oxidation on Au(111) surface populated with atomic oxygen by directly transferring its oxygen to CO to form CO_2.

EXPERIMENTAL

The experiments were performed in an ultrahigh vacuum (UHV) molecular beam surface scattering apparatus that has been described elsewhere previously,[8,56] but is briefly summarized here. The apparatus consists of a UHV scattering/analysis chamber and a quadruply differentially-pumped molecular beam source chamber. The scattering/analysis chamber (base pressure less than 2.0×10^{-10} Torr) is equipped with an Auger electron spectrometer (AES), low energy electron diffraction optics (LEED), quadrupole mass spectrometer (QMS).

The sample consists of a Au(111) single crystal (11mm in diameter, 1.5 mm thick) mounted to a tantalum plate that can be resistively heated and is in thermal contact

with a liquid nitrogen bath. Temperature of the surface is monitored with a type K thermocouple spot-welded to the sample. Oxygen atoms were deposited on the surface using a radio frequency (RF) generated plasma source that produced a supersonic beam of O atoms from an 8% (vol.) O_2 in Ar gas mixture. The oxygen atom source is a modification of a design by Pollard.[57-59] An oxygen dissociation fraction of ~40%, as measured by time of flight techniques, is achieved. Ions were deflected from the O-atom beam by a charged plate biased at 3000 V, located below the beam line in one of the differential pumping stages. The oxygen coverages were estimated by comparing the O/Au AES ratio to the O/Pt AES ratio. On Pt(111), the O/Pt ratio is 0.3 for a (2×2) oxygen adlayer composed of 3.93×10^{14} O atoms/cm^2 and a Au to Pt AES ratio of 0.95 was used as a conversion factor.[60] Here, 1ML of oxygen is defined as 1.387×10^{15} atoms/cm^2 and refers to a single atomic layer of close-packed gold.

Isotopically labeled water [$H_2{}^{18}O$] was used to distinguish the oxygen species from oxygen atom doses and water doses. Water dose is also measured in ML as with oxygen atoms. A typical value for the CO beam flux was ~9×10^{13} molecules / cm$^2\cdot$ s.

All of the beams (oxygen, water, and CO) were expanded from the same nozzle through the same apertures to ensure that the beam spots on the gold sample were the same in size and coincident. The RF generator was switched on only when it was necessary to dose atomic oxygen through the nozzle. The beam spot (~3 mm in diameter) was much smaller than the sample size to minimize effects from impinging gas interacting with other surfaces in the chamber. The Au(111) surface was cleaned by argon ion sputtering followed by annealing in UHV to eliminate carbon and other surface

impurities. The cleaning cycle was repeated until no appreciable impurity signal could be detected by AES. Surface crystallinity was verified by LEED.

RESULTS AND DISCUSSION

Oxygen and Water Interaction on Au(111)

Figure 5.1 displays a temperature programmed desorption (TPD) of isotopically labeled water [$H_2{}^{18}O$] on the Au(111) surface. Figure 5.1 (a) shows a 0.6 ML of water desorbing from clean Au(111) surface with a desorption peak temperature of 155 K. Water is known to exhibit zero-order desorption kinetics from Au(111) surface and submonolayer and multilayer water cannot be distinguished from each other clearly.[61] The spectrum is similar to those spectra previously reported from Au(111).[61] Figure 5.1 (b) shows TPD after exposure of 0.6 ML of $H_2{}^{18}O$ to 0.18 ML of oxygen covered surface at 77 K. As can be seen, the TPD spectra in Figure 5.1 (b) shows a new feature at a higher temperature (175 K) compared to the clean Au(111) surface. Figure 5.1 (c) shows TPD after exposure of 0.1 ML of $H_2{}^{18}O$ to 0.18 ML of oxygen covered surface at 77 K to show just the high temperature desorption peak feature. This second peak at 175 K is believed to be from formation of stable H_2O-O complexes on the surface which results in a higher desorption peak temperature than on pristine single crystal metal surface. It is well known that for the Au(111) surface, the metal-water interaction is much weaker than the water-water interaction and that it does not have a distinct monolayer water TPD feature as with many other metal surfaces.[61] But with the oxygen precovered surface, one can imagine that water can form a hydrogen bond with the oxygen layer and bind more

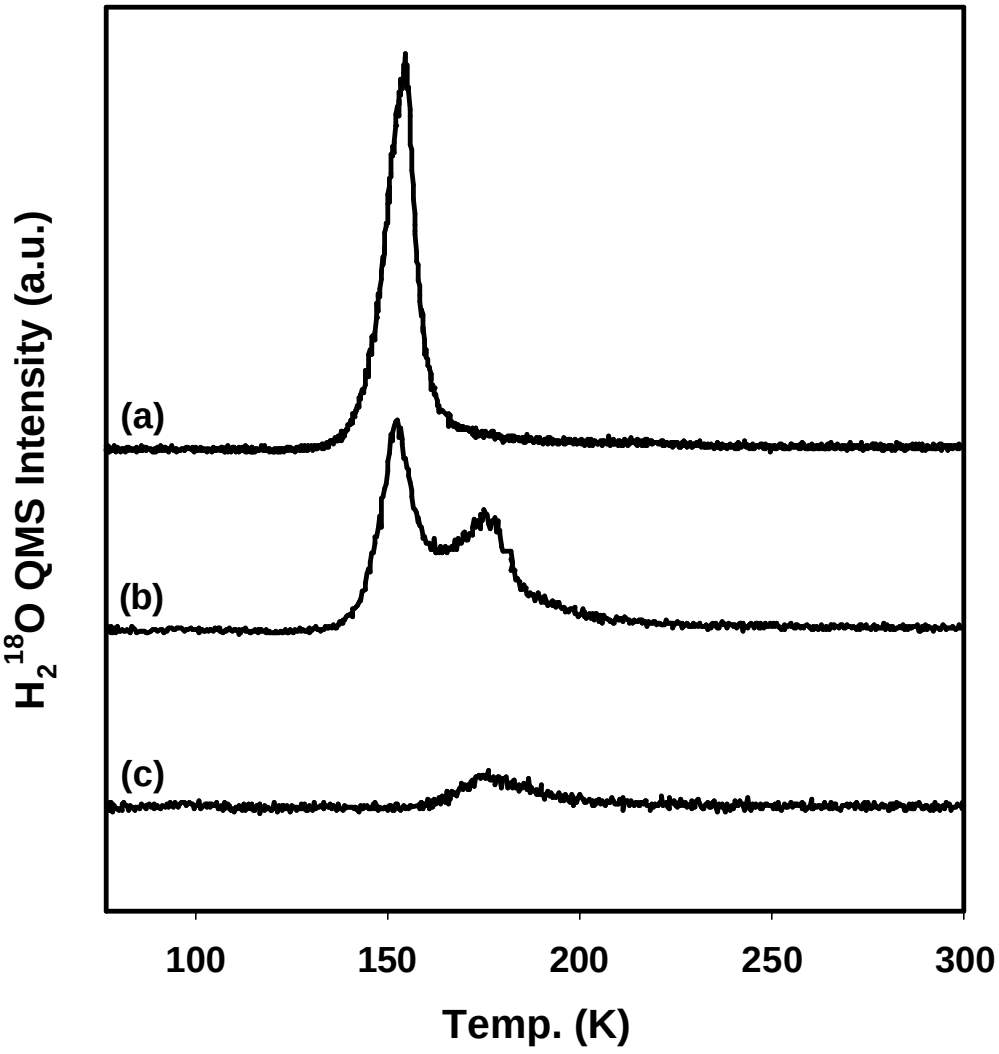

Figure 5.1: TPD of (a) 0.6 ML of $H_2{}^{18}O$ on clean Au(111) surface, (b) 0.6 ML of $H_2{}^{18}O$ on 0.18 ML of ^{16}O covered surface, and (c) 0.1 ML of $H_2{}^{18}O$ on 0.18 ML of ^{16}O covered surface. All isotopically labeled water and oxygen atoms were dosed at 77 K. Heating rate of ß = 1 K/s was used.

strongly to the surface than on clean Au(111) surface. As mentioned briefly in the introduction, based on previous study by Lazaga et al.,[49] it was considered that oxygen precovered Au(111) surface is inactive in dissociating water on the surface. They proposed that during the TPD of this surface, the H_2O-O complex decomposes to evolving water and leaves the original oxygen atom on the surface.

Figure 5.2 shows the oxygen TPD spectra of (a) 0.37 ML of ^{16}O and (b) 0.6 ML of isotopically labeled water [$H_2{}^{18}O$] dose in addition to 0.37 ML of ^{16}O. As can be seen, just with the oxygen atom dose, only mass 32 oxygen is desorbing from the surface, but when 0.6 ML of $H_2{}^{18}O$ was added on ^{16}O covered Au(111) surface, mass 34 and even mass 36 oxygen is seen to desorb from the surface in addition to mass 32 oxygen, which clearly shows that water indeed is reacting with the oxygen layer to result in scrambling of oxygen between water and preadsorbed oxygen atoms. This indicates that atomic oxygen dosed using our RF generated plasma source, especially at low temperatures, will induce activation of water or perhaps abstract hydrogen from water to create OH groups. This OH group will upon heating, recombine to form water and oxygen atom on the surface. In this process, oxygen scrambling occurs. Many metal surfaces show this kind of behavior and we will later discuss why we see a different behavior compared to results from Lazaga et al. We note that with just water on Au(111) (i.e., no preadsorbed oxygen), we see no sign of water dissociation or recombinative oxygen desorption near 535 K. Outka et al. also observed isotope mixing when they coadsorbed ^{18}O and $H_2{}^{16}O$ on Au(110) and performed a TPD.[62] They also ascribed this oxygen scrambling to either

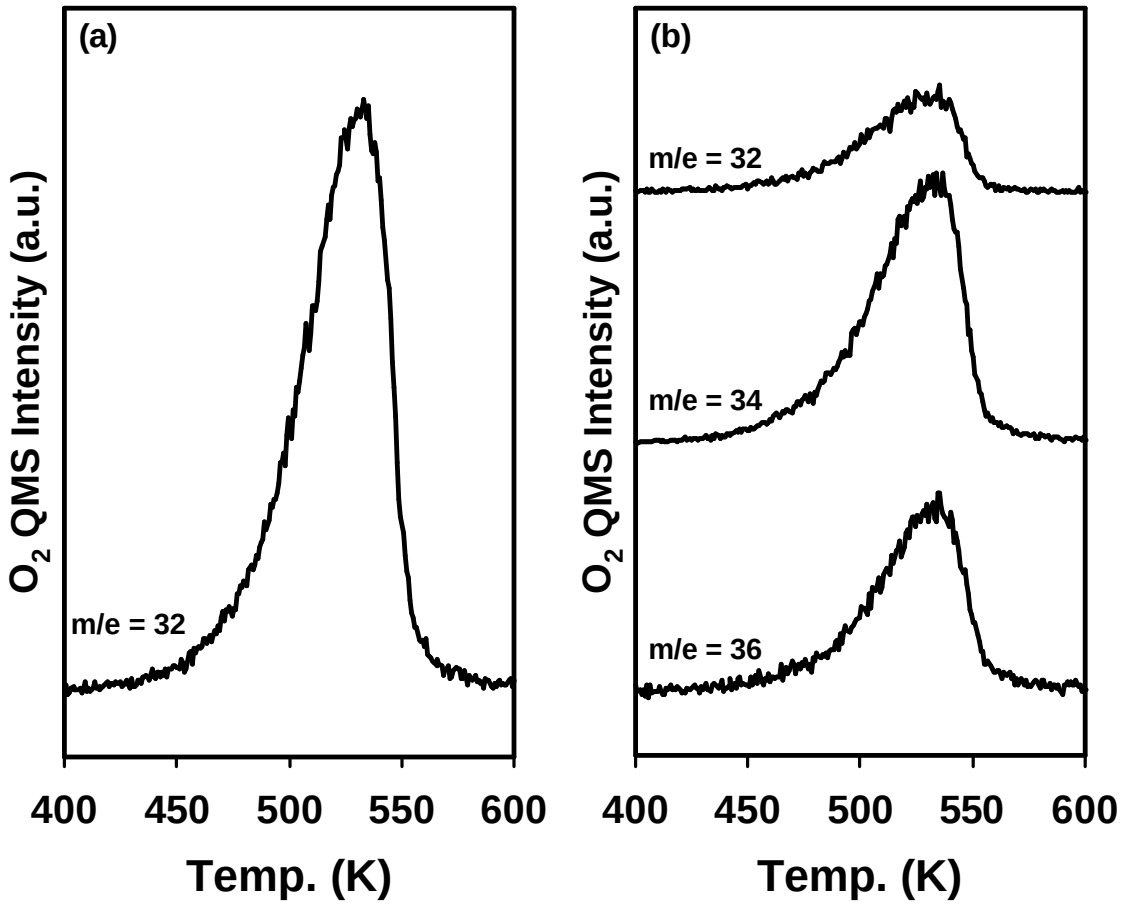

Figure 5.2: TPD of oxygen after dosing (a) 0.37 ML of ^{16}O, and (b) 0.6 ML of $H_2{}^{18}O$ in addition to 0.37 ML of ^{16}O on Au(111) surface. All isotopically labeled water and oxygen atoms were dosed at 77 K. Heating rate of ß = 3 K/s was used.

decomposition of oxygen-stabilized water or disproportionation of surface hydroxyls. In their study, they suggested the Brønsted base character of oxygen adatoms which can abstract an acidic hydrogen atom from adsorbed molecule on the group 1 B metals.[62]

During previous studies from this laboratory regarding CO oxidation on oxygen covered Au(111), the surface was sometimes annealed to 300 K after the oxygen atom dose to remove metastable oxygen and molecular oxygen. It was found that when CO was impinged on an oxygen precovered Au(111) surface that had been annealed to 300 K, it always resulted in a less CO_2 production than the surface that was not annealed. This indicates that oxygen atoms on the surface become less reactive upon annealing. So we wanted to see if there was a similar effect in oxygen mixing, when the surface was annealed to 300 K between oxygen dose and water dose. In our previous studies on CO oxidation on Au/TiO_2 surfaces, we have demonstrated that molecular oxygen exists on the surface and they can readily react with impinging CO molecules at sample temperature of 77 K.[9] But it should be noted that unlike the case of TiO_2 supported gold nanoparticles, very little molecular oxygen is seen on Au(111) surface compared to the Au/TiO_2 system, and that molecular oxygen has little effect in reacting with water or oxidizing CO on single crystal Au(111) surface.

Figure 5.3 show TPD spectra of (a) water and (b) oxygen after exposure of 0.6 ML of $H_2{}^{18}O$ to 0.18 ML of ^{16}O precovered Au(111). The sample was kept at 77 K during both the water and oxygen dose. In Figure 5.3 (a), the TPD spectra of water are shown with the signature bump around 175 K, indicative of the water-oxygen interaction. On Figure 5.3 (b), in addition to mass 32 oxygen, considerable amounts of mass 34 and 36 oxygen are seen to desorb from the surface. In Figure 5.3 (c) and (d), 0.18 ML of ^{16}O

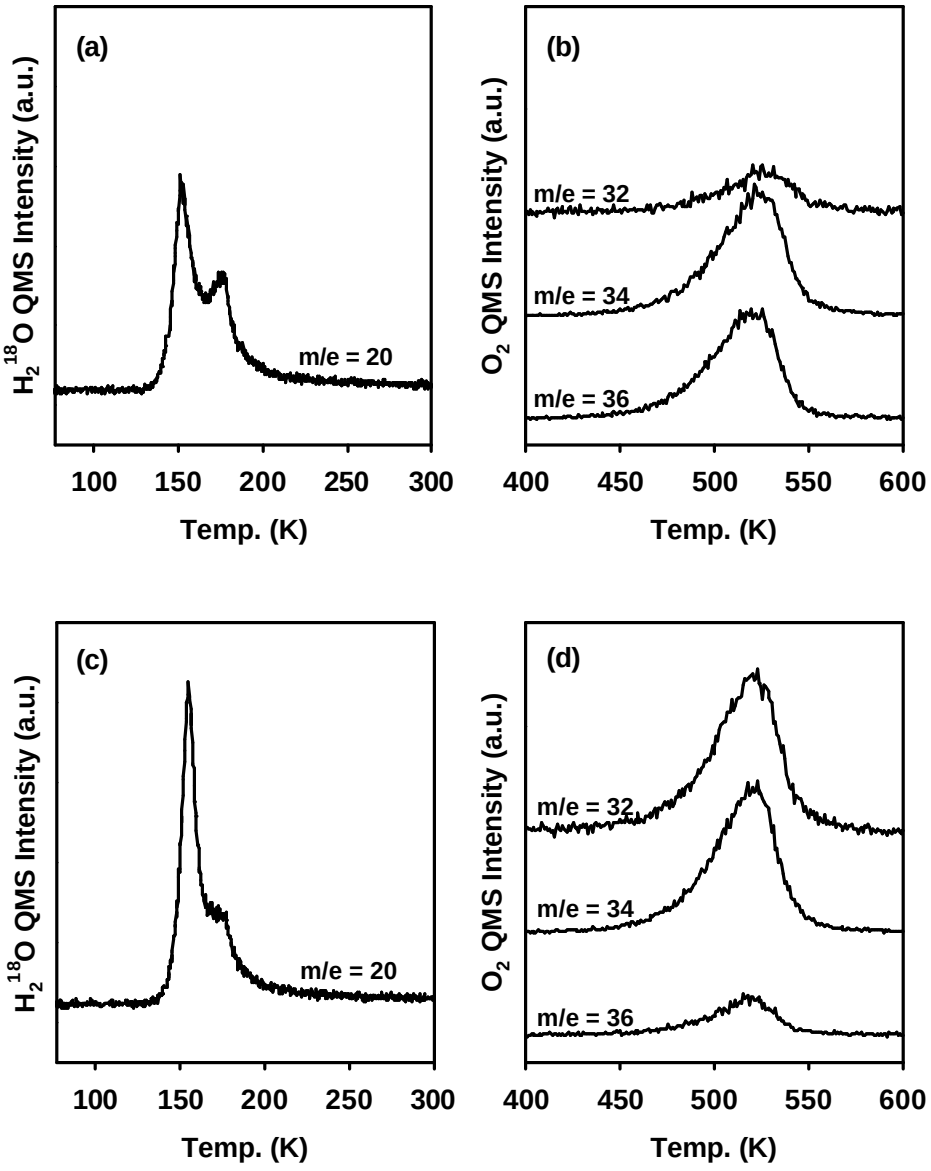

Figure 5.3: TPD of (a) $H_2{}^{18}O$ and (b) oxygen after dosing 0.6 ML of $H_2{}^{18}O$ in addition to 0.18 ML of ^{16}O on Au(111). Surface temperature was kept at 77 K during the water and oxygen dose. Heating rate of ß = 1 K/s was used for water and ß = 3 K/s for oxygen. TPD of (c) $H_2{}^{18}O$ and (d) oxygen after dosing 0.18 ML of ^{16}O on Au(111) at 77 K, and annealing the surface to 300 K(ß = 1 K/s) followed by 0.6 ML of $H_2{}^{18}O$ dose at 77 K. As in (a) and (b), heating rate of ß = 1 K/s was used for water and ß = 3 K/s for oxygen.

was dosed on Au(111) at 77 K and the surface was annealed to 300 K prior to dosing 0.6 ML of $H_2{}^{18}O$. Considering the fact that the onset of oxygen recombinative desorption occurs around 400 K, equal amount of ^{16}O is expected in both annealed and unannealed surfaces. When the surface was annealed, the portion of the water desorption features which corresponds to desorption from the clean surface increases compared to Figure 5.3 (a), and at the same time, the second feature indicative of the water-oxygen interaction considerably decreased. Finally, in Figure 5.3 (d), the amount of mass 32 which desorbs is observed to be much greater than that shown in Figure 5.3 (b) (surface unannealed), which implies less oxygen scrambling between water and oxygen atoms when the surface is annealed to 300 K prior to dosing water on the surface. We believe that annealing the surface to 300 K after oxygen dose stabilizes metastable oxygen on the surface and renders the oxygen atoms to be less reactive towards water-oxygen interaction. Therefore the difference in oxygen scrambling observed in Figure 5.3 (b) and (d) is thought to be largely due to the presence or absence of a metastable oxygen on Au(111). Studies regarding metastable oxygen on metal surface have been reviewed by Carley et al.[63] They list several examples demonstrating that reactivity of oxygen can be modified by changing the conditions under which oxygen is dosed on the metal surface. By changing the adsorption conditions for oxygen, the oxygen can be kinetically trapped in metastable state so that the reaction barrier is decreased. This metastable oxygen is what we believe is responsible for the difference in reactivity of water on oxygen precovered Au(111). As mentioned earlier, the presence of this metastable oxygen can explain the discrepancies in our results compared to the study by Lazaga et al. In their study, ozone was used to

populate the surface with atomic oxygen and all the ozone dosing was performed with the surface at 300 K.[49] This likely reduced the reactivity of surface oxygen with water.

In order to compare the effect of surface annealing on water reactivity with different oxygen coverages, we have measured the amount of mass 32 oxygen desorption in each case and compared it to oxygen desorption from a solely atomic oxygen covered surface. Take, for example, the data in Figure 5.2 with 0.37 ML of initial ^{16}O coverage, the area beneath the TPD curve in Figure 5.2 (a) would be determined and divided into the area underneath the mass 32 oxygen feature in Figure 5.2 (b). This provides a measure of how much oxygen scrambling occurs for a given oxygen dose and annealing treatment. Figure 5.4 show such data for several different initial oxygen precoverages for annealed and unannealed surfaces. In Figure 5.4, the higher the fraction of mass 32 oxygen at a given initial coverage, the less the degree of oxygen mixing. The lower curve (i.e., without annealing) shows the fraction of mass 32 oxygen desorbing with $H_2{}^{18}O$ on the surface when the surface was held at 77 K throughout the entire oxygen and water dose. The upper curve in Figure 5.4 shows the fraction of mass 32 oxygen when the surface was annealed to 300 K prior to adding $H_2{}^{18}O$ to the surface.

Clearly, the degree of mixing is always smaller for the surface which has been annealed to 300 K prior to the water dose. Apparently the water is less likely to interact dissociatively with the more stable oxygen layer created once the surface is annealed to 300 K, and this leads to less oxygen scrambling on the surface.

In both cases (with and without annealing to 300 K), the fraction of mass 32 is seen to increase as the amount of oxygen ^{16}O dose increases. The reason for this kind of behavior is believed to be due to the fact that when the surface is covered with more

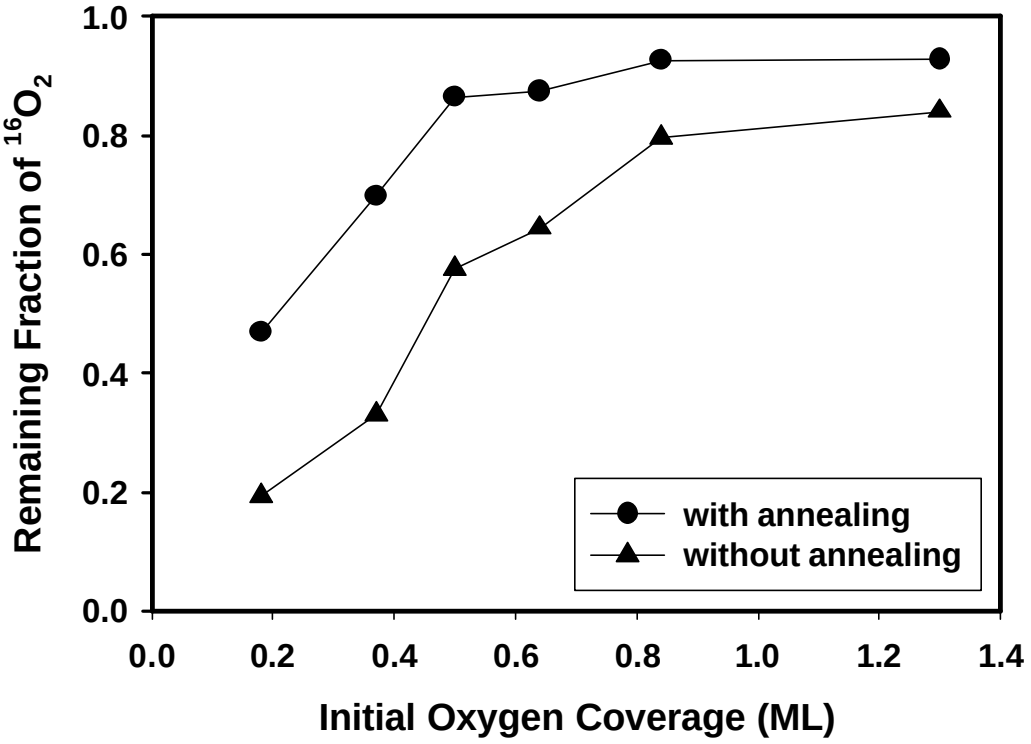

Figure 5.4: Remaining fraction of mass 32 oxygen when TPD was performed after dosing different amount (0.18, 0.37, 0.50, 0.64, 0.84, and 1.30 ML) of ^{16}O and adding 0.6 ML of $H_2{}^{18}O$ on the surface. Amount of mass 32 oxygen desorption was compared with the oxygen TPD with the corresponding ^{16}O coverage without adding any $H_2{}^{18}O$ on the surface. Lower curve shows the fraction of mass 32 oxygen desorbing when surface was not annealed to 300 K before adding $H_2{}^{18}O$. Upper curve shows the fraction of mass 32 oxygen when the surface was annealed to 300 K between ^{16}O dose and $H_2{}^{18}O$ dose on the surface.

atomic oxygen, less adsorption sites are available for water to interact with the oxygen layer, hence less oxygen scrambling. As can be seen, remaining fraction of mass 32 does not quite reach 1.0 with more than 1 ML of ^{16}O coverage, but this is believed to be due to a small concentration of defects on the surface, that can still promote water-oxygen interaction even at higher oxygen coverages.

CO Oxidation by Activated Water on Au(111)

We have recently studied low temperature CO oxidation on Au(111) and also on gold nanoparticles supported on TiO_2(110). Here we expand our studies of low temperature CO oxidation by including water as a coadsorbate on the surface. These experiments were inspired by results in which moisture was observed to enhance low temperature CO oxidation on metal oxide supported gold nanoclusters.[55,64]

Figure 5.5 demonstrates how CO reacts with oxygen originating from adsorbed water on Au(111) at 77 K. In Figure 5.5 (a), a beam of CO is impinged between 10 and 20 seconds on a 0.18 ML of ^{16}O covered surface. As shown in Figure 5.5 (a), only mass 44 $C^{16}O^{16}O$ is seen during the CO impingement. In Figure 5.5 (b), the CO beam is impinged on Au(111) with 0.1 ML of isotopically labeled $H_2{}^{18}O$. Without preadsorbed oxygen, CO does not interact with the adsorbed water to form mass 46 $C^{16}O^{18}O$ from the surface. In Figure 5.5 (c), 0.1 ML of $H_2{}^{18}O$ is dosed after a 0.18 ML exposure of ^{16}O on Au(111), followed by impingement of the CO beam. As can be seen from the data in Figure 5.5 (c), in addition to mass 44 $C^{16}O^{16}O$ which is created from CO reacting with ^{16}O on the surface, a small amount of mass 46 $C^{16}O^{18}O$ is observed, indicating that

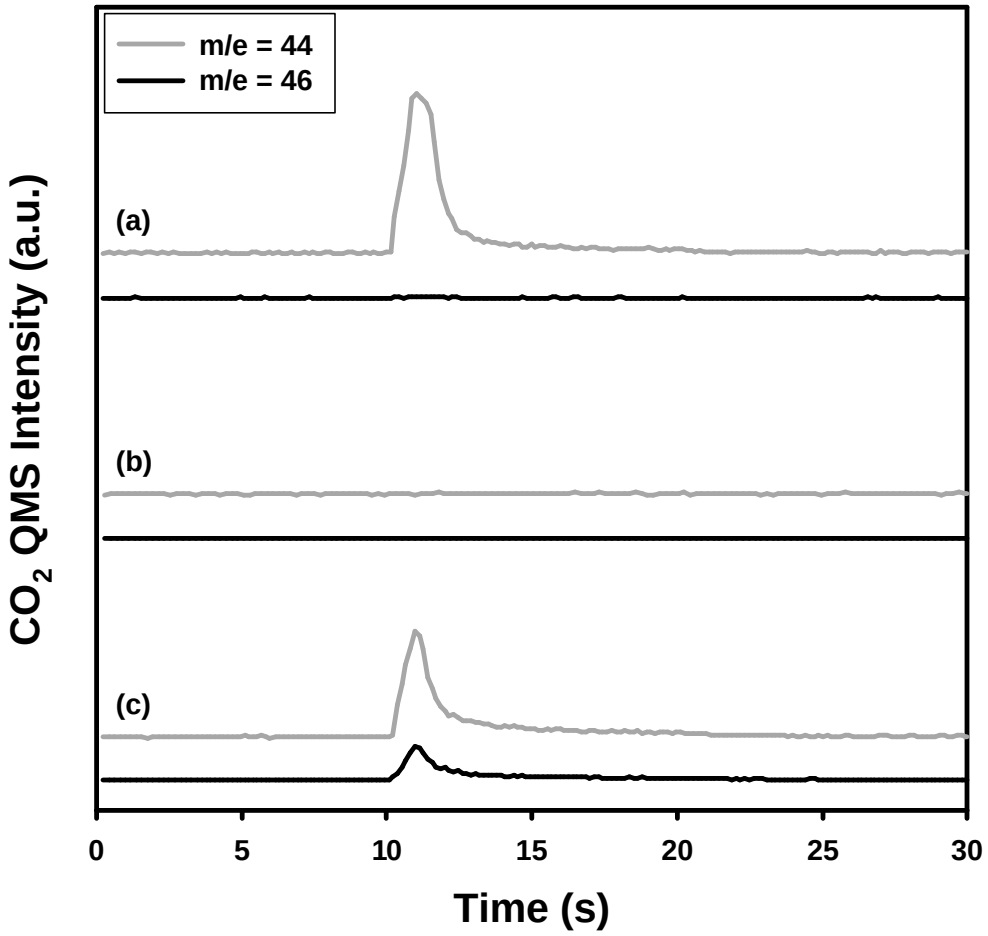

Figure 5.5: Evolution of CO_2 at 77 K while impinging a continuous CO beam (from 10 to 20 sec.) at the surface. The grey curve represents mass 44 $C^{16}O^{16}O$ and the black curve represents mass 46 $C^{16}O^{18}O$ with (a) 0.18 ML of ^{16}O atoms preadsorbed, (b) 0.1 ML of $H_2{}^{18}O$ preadsorbed, and (c) 0.1 ML of $H_2{}^{18}O$ in addition to 0.18 ML of ^{16}O atoms preadsorbed on Au(111) at 77 K. All the procedure was done while the surface temperature was kept at 77 K.

oxygen originating from water is directly involved in CO oxidation at 77 K on Au(111) when atomic oxygen is preadsorbed on the surface. A notable feature of these QMS spectra is that the CO_2 signal decays quickly (2-3 seconds), although CO beam continues to strike the surface for 10 seconds. Based on the TPD measurements following these experiments, there is still a considerable amount of surface oxygen left on the surface as well as CO. We believe that this rapid decay of CO_2 production is due to unreacted CO covering the surface, which limits further reaction at 77 K.

From the results shown in Figure 5.5, we speculate that mass 46 CO_2 may be formed by CO reacting with either activated water or hydroxyls on the surface. Although we cannot confirm the exact nature of the activated water on the surface, we note that formation of hydroxyl groups by adding water to an oxygen overlayer on a transition metal at low temperature is not uncommon. Sueyoshi et al. have shown that on Cu(100), oxygen atoms can abstract hydrogen from water to form hydroxyls at temperatures as low as 100 K based on their HREELS study.[65] And similar reaction may take place on Au(111), especially with metastable oxygen species on the surface.

The reaction of CO and OH leading to CO_2 formation is widely studied in gas phase chemistry due to the pivotal role of OH radicals in atmospheric chemistry.[66,67] There are also many investigations of CO and OH reaction on metal surfaces, mostly related to electrochemistry.[68-70] One relevant study regarding the reaction of adsorbed CO and OH on Pt(111) under UHV conditions was performed by Bergeld et al.[70] This study showed that water can promote CO oxidation on oxygen covered Pt(111). They observed that a previously unobserved CO_2 desorption peak around 200 K appears when water was coadsorbed prior to temperature programmed reaction of a Pt(111) surface

populated with CO and atomic oxygen. This new peak occurs at a much lower temperature than the CO_2 desorption peak (~300 K) for a typical CO reaction with oxygen adatom peak and it has been attributed to CO reacting with OH groups on the surface. It is possible that a similar reaction can occur on Au(111) in which hydroxyls are formed from water splitting and reacting with CO to form CO_2 at 77 K. Related calculations were performed by Gong et al. who found that on Pt(111), the CO_2 formation is likely to follow a mechanism in which CO first reacts with OH to form surface COOH and this COOH further reacts with OH to form CO_2 and H_2O.[71]

In order to gain more information about low temperature CO oxidation, oxygen precoverage was varied while keeping the amount of water dose constant. Figure 5.6 shows CO oxidation by coadsorbed oxygen and water on Au(111) at a temperature of 77 K at different oxygen coverages. Again, CO beam was impinged on the sample between 10 and 20 seconds in these experiments. Oxygen coverages were (a) 0.08 ML, (b) 0.18 ML, (c) 0.50 ML, (d) 0.84 ML, with a water exposure of 0.1 ML for all cases. As seen in Figure 5.5, both mass 44 and mass 46 CO_2 are produced from impinging CO on the surface. On the right, in the bar chart, the amount of CO_2 produced is shown beside the corresponding CO_2 QMS signal. On the far right, the mass 46 CO_2 production to mass 44 CO_2 production ratio is shown for each experiment. As the ^{16}O coverage increases, the mass 44 CO_2 production increases accordingly with additional availability of oxygen on the surface. But when oxygen precoverage reaches higher value, the mass 44 CO_2 production is greatly decreased due to the site blocking by both oxygen and water. Mass 46 CO_2 production illustrates a similar behavior where the CO_2 production peaks and decreases as the amount of preadsorbed oxygen increases. With 0.84 ML of preadsorbed

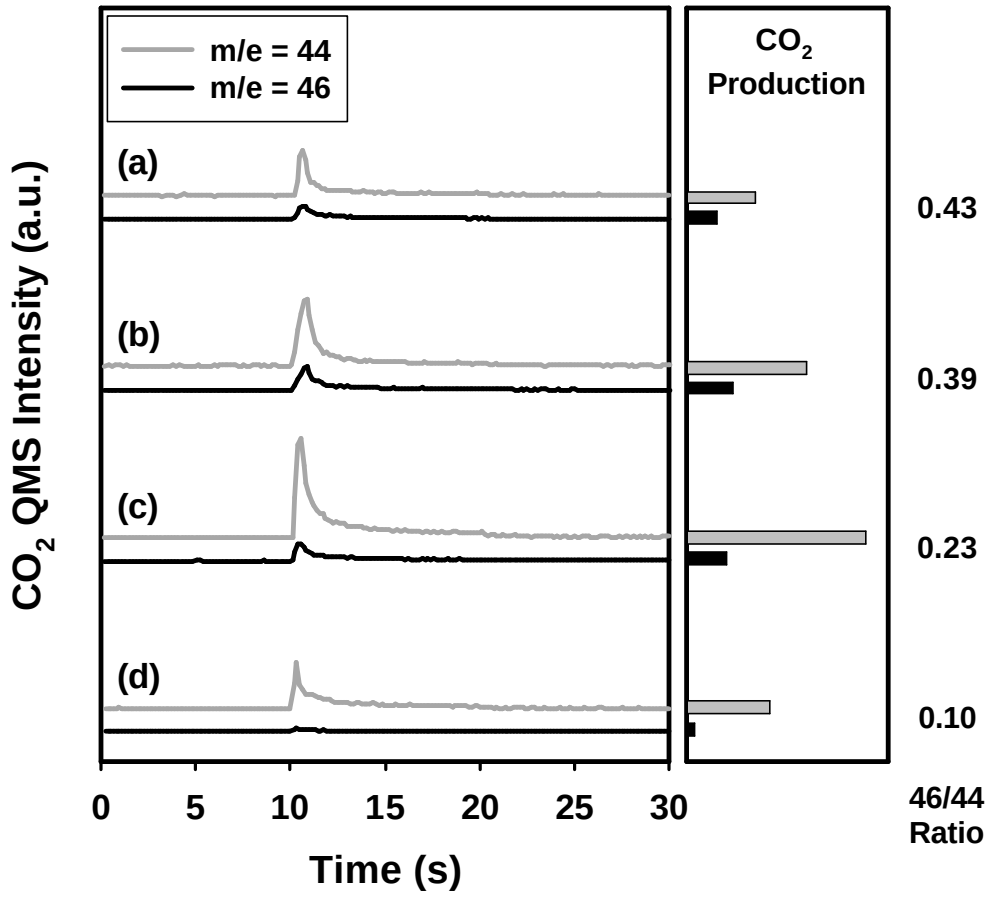

Figure 5.6: Evolution of CO_2 at 77 K while impinging a continuous CO beam (from 10 to 20 sec.) at the surface with different oxygen coverage and 0.1 ML of $H_2{}^{18}O$ on the surface. The grey curves represent mass 44 $C^{16}O^{16}O$ and the black curves represent mass 46 $C^{16}O^{18}O$ with (a) 0.08 ML, (b) 0.18 ML, (c) 0.50 ML, and (d) 0.84 ML of ^{16}O atoms preadsorbed on Au(111) surface at 77 K. On the right in the bar chart, relative amount of CO_2 produced in each case is shown next to the corresponding QMS spectra. On the far right, mass 46 to mass 44 CO_2 production ratio is shown for each oxygen coverage. All the procedure was done while the surface temperature was kept at 77 K.

oxygen, there is very little mass 46 CO_2 produced. With increasing oxygen precoverage, the ratio of mass 46 to mass 44 decreases until it reaches 0.10 for 0.84 ML of oxygen precoverage. This is because water has less opportunity to find an open site on the surface to interact with oxygen atoms as the oxygen coverage increases. This results in less oxygen originating from water for CO to react with and less mass 46 CO_2 production relative to mass 44 CO_2 production.

In order to further explore CO_2 production from adsorbed water, we compared the total amount of CO_2 produced from a solely oxygen covered Au(111) surface with that of a Au(111) surface covered with both atomic oxygen and water. As mentioned earlier, not all of the adsorbed oxygen is consumed when a CO beam is impinged on the surface at 77 K due to accumulation of adsorbed CO. In order to avoid this situation, we have conducted additional experiments at T_s = 140K, a temperature well below the desorption peak temperature (175 K) of water on oxygen covered Au(111) but above the desorption peak temperature (108 K) for CO. This was done to keep the surface coverage of CO low in order not to limit the reaction by surface accumulation of CO and also to keep the water coverage unaffected throughout the reaction. Although not shown here, we note that water alone will not oxidize CO even at 140 K.

In Figure 5.7 (a), a CO beam is impinged on a 0.08 ML of ^{16}O covered surface at 140 K. The area underneath the curve between 10 and 40 seconds represents the amount of mass 44 CO_2 produced as shown in the inset. As expected, no mass 46 CO_2 is detected in this case. In Figure 5.7 (b), a CO beam is impinged on a surface where 0.08 ML of ^{16}O is dosed first and 0.1 ML of $H_2{}^{18}O$ is added afterwards. The grey curve represents the amount of mass 44 CO_2 production and the black curve represents the

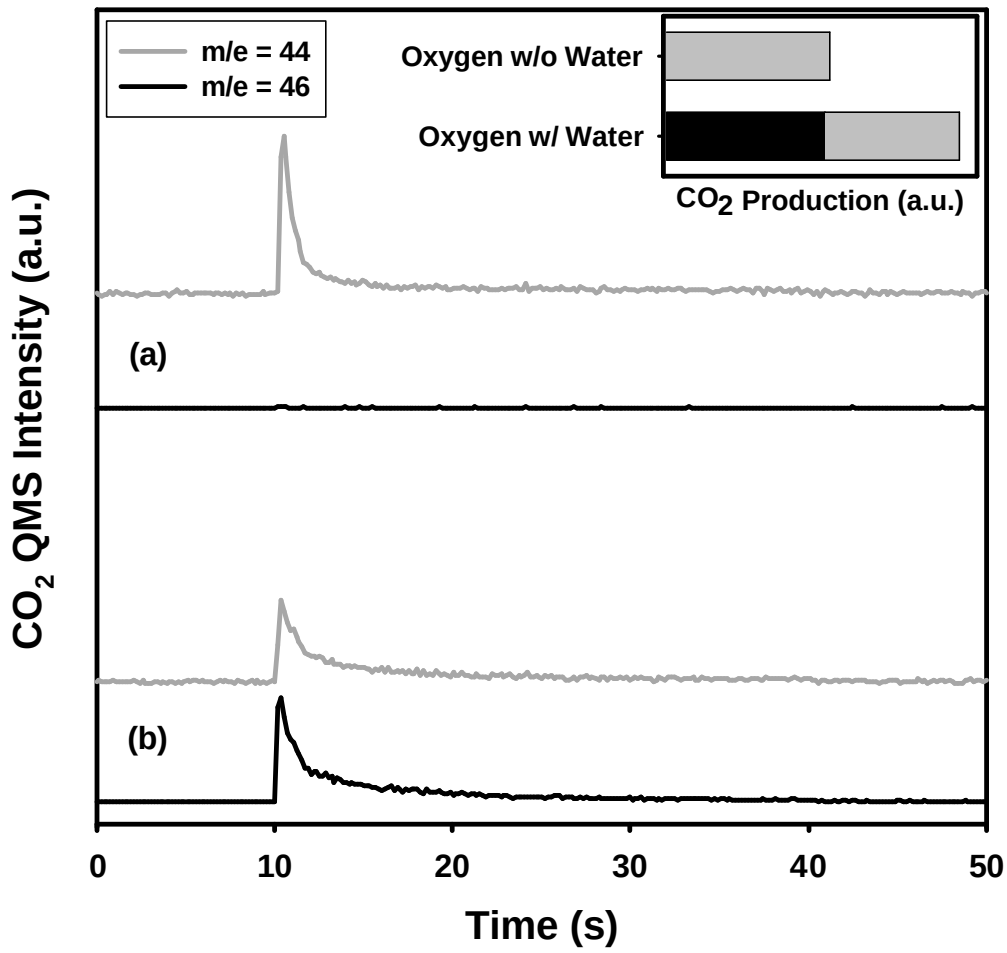

Figure 5.7: Evolution of CO_2 at 140 K while impinging a continuous CO beam (from 10 to 40 sec.) at the surface. Grey curve represents mass 44 $C^{16}O^{16}O$ and black curve represents mass 46 $C^{16}O^{18}O$ with (a) 0.08 ML of ^{16}O preadsorbed, (b) 0.1 ML $H_2{}^{18}O$ in addition to 0.08 ML of ^{16}O atoms preadsorbed on Au(111) at 77 K. The area underneath the curve between 10 and 40 seconds represent the amount of CO_2 produced as shown in the inset.

amount of mass 46 CO_2 produced during the CO impingement. The inset shows the total amount of CO_2 produced for each case in a bar chart, with the grey bar representing mass 44 CO_2 and the black bar representing mass 46 CO_2. As shown, much more CO_2 production is observed when water is added to the oxygen layer on the surface. This is similar to what Bergeld et al. have observed on Pt(111) where they demonstrated the promotional effect of water on CO oxidation.[70] Based on the TPD measurements afterwards (not shown here), there was no appreciable amount of oxygen left on the surface after the CO impingement at 140K. However a small amount of $H_2{}^{18}O$ and $H_2{}^{16}O$ (this comes from oxygen scrambling between ^{16}O and $H_2{}^{18}O$ to produce $H_2{}^{16}O$) was observed that was not consumed during the reaction. Once the oxygen atoms that activate water are completely consumed either by directly reacting with CO or reacting with CO as hydroxyls, the remaining water on the surface does not react with CO. This is in agreement with the results shown in Figure 5.5 (b) where it was shown that water alone cannot oxidize CO when atomic oxygen is consumed by reaction and thereby unable to activate water. From these results we speculate that either activated water or OH groups formed from water interacting with atomic oxygen on Au(111) participate in oxidizing CO to produce CO_2 on the surface.

If the mass 46 CO_2 in Figure 5.7 was just from CO reacting with atomic oxygen which maybe formed from isotopically labeled $H_2{}^{18}O$ transferring its hydrogen atoms to nearby ^{16}O atoms, we would expect to see an equal amount of CO_2 produced compared to the surface without adsorbed water, because there would still be approximately the same amount of atomic oxygen on the surface even if hydrogen from water moved from ^{18}O to

^{16}O. But we clearly see an increase in total amount of CO_2 produced, which indicates that water is activated by atomic oxygen on the surface to take part in CO oxidation.

It is also possible to argue that this extra amount of CO_2 is produced from additional oxygen atoms created by complete dissociation of water on the oxygen covered surface. In this case, water may lose a hydrogen atom to a nearby oxygen atom and the resulting OH groups further dissociate on the surface to leave oxygen atoms on the surface. But, it is well known that on metals that does not dissociate water on clean surfaces, which includes Au(111) surface, OH dissociation is not favored over two OH groups recombining to form one water and leave an oxygen atom on the surface.[42] So we can also rule out the possibility of additional amount of oxygen on the surface being responsible for the extra amount of CO_2 produced on the surface. We note that although we tried to account for hydrogen from the reaction, we have yet to detect hydrogen or hydrogen containing species, such as H_2CO, during the CO impingement or subsequent TPD.

Over the course of our experiments, we found that not only does water enhance CO oxidation by supplying extra oxygen, but as shown in Figure 5.8, water also seems to keep metastable oxygen adatoms from becoming more stable oxygen species on the surface. This in turn seems to keep the reactivity of adsorbed oxygen higher than when there is no water on the surface.

Figure 5.8 demonstrates how water helps retain the reactivity of metastable oxygen adatoms on Au(111). For Figures (a) and (c), the grey curve represents the amount of mass 44 CO_2 production and the black curve represents the amount of mass 46 CO_2 produced during the CO impingement. The insets show the total amount of CO_2

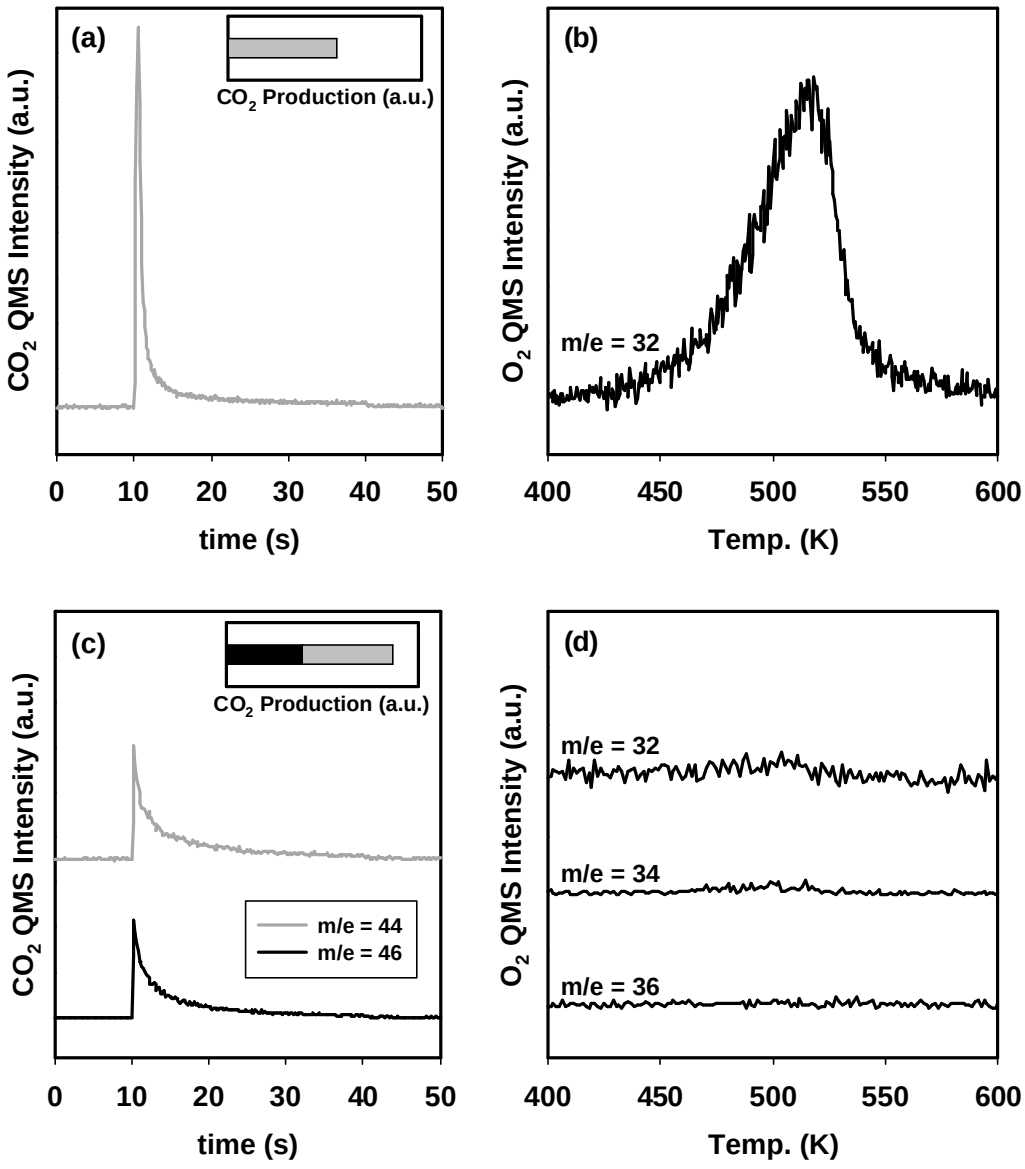

Figure 5.8: Evolution of CO_2 at 140 K while impinging a continuous CO beam (from 10 to 40 sec.) at the surface. Grey curve represents mass 44 $C^{16}O^{16}O$ and black curve represents mass 46 $C^{16}O^{18}O$ with (a) 0.18 ML of ^{16}O preadsorbed, (c) 0.1 ML $H_2{}^{18}O$ in addition to 0.18 ML of ^{16}O atoms preadsorbed on Au(111) at 77 K. The area underneath the curve between 10 and 40 seconds represent the amount of CO_2 produced as shown in the inset. (b) and (d) shows the respective oxygen TPD afterwards (ß = 3 K/s).

produced for each case in bar chart with the corresponding color for mass 44 and 46 CO_2. Figure 5.8 (a) shows CO_2 production at sample temperature of 140 K with 0.18 ML of ^{16}O on the surface. Figure 5.8 (b) is the oxygen TPD following (a). As can be seen, 30 sec CO beam exposure was not enough to consume all the oxygen on the surface. As stated earlier, annealing the surface to 300 K resulted in less reactive oxygen layer on the surface. Although surface is not annealed up to 300 K in this case, we can imagine that some of the metastable oxygen may have enough thermal energy to stabilize themselves on the surface. We believe that some of these stable oxygen species are what we observe during the TPD on Figure 5.8 (b). On Figure 5.8 (c), CO is impinged on top of 0.1 ML of $H_2{}^{18}O$ and 0.18 ML of ^{16}O covered surface at 140 K. Insets in (a) and (c) shows the total amount of CO_2 production and as expected, total CO_2 production was greater for the surface with water and oxygen (as shown in the in. Interestingly, in the following TPD (Figure 5.8 (d)), no detectable oxygen was observed. This result indicates that all the oxygen was consumed during the CO impingement and that when water is added to the oxygen layer, it can promote the reactivity of oxygen atoms on the surface by inhibiting metastable oxygen from stabilizing to the surface. In a study by Davies et al., they observed that oxygen atoms can be prevented from forming a more stable $O^{2-}_{(a)}$ state by coadsorbed NH_3 on Cu(111) surface.[72] We believe a similar argument can be made with water in our case. It is plausible that metastable oxygen can be kept from forming more stable oxygen state on the surface by water, hence retaining higher reactivity towards CO at 140 K.

We note that even if we account for all the remaining oxygen in Figure 5.8 (b), and assume they all reacted with CO to produce CO_2, the total amount of CO_2 produced

with water in addition to oxygen would still be 15 % greater than CO_2 production with just oxygen on the surface.

CONCLUSIONS

We have presented results of an investigation into the interaction of water with oxygen atoms preadsorbed on Au(111) surface. We have shown that when our RF generated plasma source is used to generate and deposit oxygen atoms, water can interact with oxygen atoms on the Au(111) surface resulting in oxygen scrambling on the surface. We also addressed the role of metastable oxygen state present in our experiments that accounts for previously unobserved reactivity of water on oxygen covered Au(111). These metastable oxygen species are shown to be much more reactive than stable oxygen layer towards water to cause oxygen scrambling between water and oxygen adatoms.

We have also shown that water can directly participate in oxidizing CO on oxygen covered Au(111) surface. It was shown that addition of water on oxygen covered Au(111) can greatly increase the amount of CO_2 production at low temperatures. From these results, we speculate that either activated water or OH groups formed from water interacting with atomic oxygen on Au(111) can participate in oxidizing CO to produce CO_2 on the surface. It was also demonstrated that while annealing the surface to 300 K can stabilize the metastable oxygen dosed at surface temperature of 77 K on Au(111), adding water immediately after dosing oxygen atoms on the surface can keep metastable oxygen adatoms from becoming more stable on the surface. This in turn seems to keep the reactivity of adsorbed oxygen higher than when there is no water on the surface.

REFERENCES

1. G. C. Bond, D. T. Thompson, Catal. Rev. – Sci. Eng. **41**, 319 (1999).

2. M. Haruta, T. Kobayashi, H. Sano, N. Yamada, Chem. Lett. 405 (1987).

3. S. D. Lin, M. Bollinger, M. A. Vannice, Catal. Lett. **17**, 245 (1993).

4. S. Tsubota, D. A. H. Cunningham, Y. Bando, M. Haruta, Stud. Surf. Sci. Catal. **91**, 227 (1995).

5. W. S. Epling, G. B. Hoflund, J. F. Weaver, S. Tsubota, M. Haruta, J. Phys. Chem. **100**, 9929 (1996).

6. B. Schumacher, V. Plzak, M. Kinne, R. J. Behm, Catal. Lett. **89**, 109 (2003).

7. S. T. Daniells, M. Makkee, J. A. Moulijn, Catal. Lett. **100**, 39 (2005).

8. T. S. Kim, J. D. Stiehl, C. T. Reeves, R. J. Meyer, C. B. Mullins, J. Am. Chem. Soc. **125**, 2018 (2003).

9. J. D. Stiehl, T. S. Kim, S. M. McClure, C. B. Mullins, J. Am. Chem. Soc. **126**, 13574 (2004).

10. E. E. Stangland, K. B. Stavens, R. P. Andres, W. N. Delgass, J. Catal. **191**, 332 (2000).

11. T. Hayashi, K. Tanaka, M. Haruta, J. Catal. **178**, 566 (1998).

12. G. Mul, A. Zwijnenburg, B. van der Linden, M. Makkee, J. A. Moulijn, J. Catal. **201**, 128 (2001).

13. Q. Fu, H. Saltsburg, M. Flytzani-Stephanopoulos, Science **301**, 935 (2003).

14. Z.-P. Liu, S. J. Jenkins, D. A. King, Phys Rev. Lett. **94**, 196102. (2005).

15. D. Andreeva, V. Idakiev, T. Tabakova, L. Ilieva, P. Falaras, A. Bourlinos, A. Travlos, Catal. Today **72**, 51 (2002).

16. M. M. Schubert, S. Hackenberg, A. C. van Veen, M. Muhler, V. Plzak, R. J. Behm, J. Catal. **197**, 113 (2001).

17. M. A. Bollinger, M. A. Vannice, Appl. Catal. B: Environ. **8**, 417 (1996).

18. J.-D. Grunwaldt, A. Baiker, J. Phys. Chem. B **103**, 1002 (1999).

19. H. M. Ajo, V. A. Bondzie, C. T. Campbell, Catal. Lett. **78**, 359 (2002).

20. Z.-P. Liu, P. Hu, A. Alavi, J. Am. Chem. Soc. **124**, 14770 (2002).

21. Y. Xu, M. Mavrikakis, J. Phys. Chem. B **107**, 9298 (2003).

22. G. Mills, M. S. Gordon, H. Metiu, J. Chem. Phys. **118**, 4198 (2003).

23. H. G. Boyen, G. Kaestle, F. Weigl, B. Koslowski, C. Dietrich, P. Ziemann, J. P. Spatz, S. Riethmueller, C. Hartmann, M. Moeller, G. Schmid, M. G. Garnier, P. Oelhafen, Science **297**, 1533 (2002).

24. N. Lopez, J. K. Norskov, J. Am. Chem. Soc. **124**, 11262 (2002).

25. N. A. Hodge, C. J. Kiely, R. Whyman, M. R. H. Siddiqui, G. J. Hutchings, Q. A. Pankhurst, F. E. Wagner, R. R. Rajaram, S. E. Golunski, Catal. Today **72**, 133 (2002).

26. R. M. Finch, N. A. Hodge, G. J. Hutchings, A. Meagher, Q. A. Pankhurst, M. R. H. Siddiqui, F. E. Wagner, and R. Whyman, Phys. Chem. Chem. Phys. **1**, 485 (1999).

27. A. M. Baro, W. Erley, J. Vac. Sci. Technol. **20**, 580 (1982).

28. B. W. Callen, K. Griffiths, P. R. Norton, D. A. Harrington, J. Phys. Chem. **96**, 10905 (1992).

29. J. E. Crowell, J. G. Chen, D. M. Hercules, J. T. Yates, Jr., J. Chem. Phys. **86**, 5804 (1987).

30. P. Jiang, M. W. Zappone, S. L. Bernasek, A. Robertson, Jr., J. Vac. Sci. Technol. A **14**, 2372 (1996).

31. Y. Shao, J. Paul, Appl. Surf. Sci. **72**, 113 (1993).

32. A. Spitzer, H. Lueth, Surf. Sci. **160**, 353 (1985).

33. C. T. Au, A. F. Carley, A. Pashuski, S. Read, M. W. Roberts, A. Zeini-Isfahan, Springer Ser. Surf. Sci. **33**, 241 (1993).

34. K. Bedurftig, S. Volkening, Y. Wang, J. Wintterlin, K. Jacobi, G. Ertl, J. Chem. Phys. **111**, 11147 (1999).

35. J. R. Creighton, J. M. White, Surf. Sci. **136**, 449 (1984).

36. M. Klaua, T. E. Madey, Surf. Sci. **136**, L42 (1984).

37. A. P. Seitsonen, Y. Zhu, K. Beduerftig, H. Over, J. Am. Chem. Soc. **123**, 7347 (2001).

38. K. Bange, T. E. Madey, J. K. Sass, E. M. Stuve, Surf. Sci. **183**, 334 (1987).

39. G. B. Fisher, B. A. Sexton, Phys. Rev. Lett. **44**, 683 (1980).

40. J. Kubota, J. Kondo, K. Domen, C. Hirose, Surf. Sci. **295**, 169 (1993).

41. C. Nyberg, C. G. Tengstaal, J. Chem. Phys. **80**, 3463 (1984).

42. M. A. Henderson, Surf. Sci. Rep. **46**, 1 (2002).

43. D. L. Doering, T. E. Madey, Surf. Sci. **123**, 305 (1982).

44. K. Kretzschmar, J. K. Sass, P. Hofmann, A. Ortega, A. M. Bradshaw, S. Holloway, Chem. Phys. Lett. **78**, 410 (1981).

45. T. E. Madey, J. T. Yates, Jr., Chem. Phys. Lett. **51**, 77 (1977).

46. T. Pache, H. P. Steinrueck, W. Huber, D. Menzel, Surf. Sci. **224**, 195 (1989).

47. M. Schulze, R. Reissner, K. Bolwin, W. Kuch, Fresen. J. Anal. Chem. **353**, 661 (1995).

48. P. A. Thiel, F. M. Hoffmann, W. H. Weinberg, Phys. Rev. Lett. **49**, 501 (1982).

49. M. A. Lazaga, D. T. Wickham, D. H. Parker, G. N. Kastanas, B. E. Koel, ACS Sym. Ser. **523**, 90 (1993).

50. C. T. Au, M. W. Roberts, Proc. Roy. Soc. London, Ser. A **396**, 165 (1984).

51. C. T. Au, M. W. Roberts, A. R. Zhu, J. Chem. Soc., Chem. Commun. 737 (1984).

52. A. F. Carley, P. R. Davies, M. W. Roberts, K. K. Thomas, Surf. Sci. **238**, L467 (1990).

53. A. F. Carley, P. R. Davies, M. W. Roberts, N. Shukla, Y. Song, K. K. Thomas, Appl. Surf. Sci. **81**, 265 (1994).

54. G. U. Kulkarni, C. N. R. Rao, M. W. Roberts, Langmuir **11**, 2572 (1995).

55. M. Date, M. Okumura, S. Tsubota, M. Haruta, Angew. Chem. –Int. Edit. **43**, 2129 (2004).

56. M. C. Wheeler, D. C. Seets, C. B. Mullins, J. Chem. Phys. **105**, 1572 (1996).

57. J. E. Pollard, Rev. Sci. Instrum. **63**, 1771 (1992).

58. M. C. Wheeler, C. T. Reeves, D. C. Seets, C. B. Mullins, J. Chem. Phys. **108**, 3057 (1998).

59. M. C. Wheeler, D. C. Seets, C. B. Mullins, J. Chem. Phys. **107**, 1672 (1997).

60. D. A. Outka, R. J. Madix, Surf. Sci. **179**, 351 (1987).

61. B. D. Kay, K. R. Lykke, J. R. Creighton, S. J. Ward, J. Chem. Phys. **91**, 5120 (1989).

62. D. A. Outka, R. J. Madix, J. Am. Chem. Soc. **109**, 1708 (1987).

63. A. F. Carley, P. R. Davies in *Interfacial Science*, edited by M. W. Roberts (Blackwell, Oxford, 1997).

64. M. Date, M. Haruta, J. Catal. **201**, 221 (2001).

65. T. Sueyoshi, T. Sasaki, Y. Iwasawa, J. Phys. Chem. B **101**, 4648 (1997).

66. T. Rockmann, C. A. M. Brenninkmeijer, G. Sauerssig, P. Bergamaschi, J. N. Crowley, H. Fischer, P. J. Cruutzen, Science **281**, 544 (1998).

67. M. I. Lester, B. V. Pond, D. T. Anderson, L. B. Harding, A. F. Wagner, J. Chem. Phys. **113**, 9889 (2000).

68. B. E. Hayden, M. E. Rendall, O. South, J. Am. Chem. Soc. **125**, 7738 (2003).

69. T. Lei, M. S. Zei, G. Ertl, Surf. Sci. **581**, 142 (2005).

70. J. Bergeld, B. Kasemo, D. V. Chakarov, Surf. Sci. **495**, L815 (2001).

71. X.-Q. Gong, P. Hu, R. Raval, J. Chem. Phys. **119**, 6324 (2003).

72. P. R. Davies, M. W. Roberts, N. Shukla, D. J. Vincent, Surf. Sci. **325**, 50 (1995).

Chapter 6: Concluding Remarks

The field of gold catalysis has been gaining enormous popularity during the last two decades. The fact that gold is inert in a bulk form but shows an extraordinary reactivity once the particle size is decreased to nanometer size range makes it a perfect research target for many scientists to study the fundamental aspects of nanomaterials. In addition, due to the natural abundance of gold over other platinum group metals and its lower price, gold as a catalyst material is a very attractive option for economical reasons.[1] From the rich chemistry gold provides in oxidation reactions, it is evident that we can expect to see much more exciting discoveries in the near future. On the other hand, in order for gold to be commercially useful, there are many issues that need to be resolved. The nature of active sites will have to be clarified and detailed mechanisms will need to be explained in order to design a good catalyst. Also, making a durable catalyst by improving the sintering characteristics will be another great challenge. Nevertheless, a low activation energy of reaction and the positive effect of moisture makes gold catalysts a prime candidate for many environmental applications at ambient conditions such as automotive pollution control.[2] In this dissertation, Au/TiO_2 and Au(111) were used to answer some of the basic aspects of gold catalysis by focusing on CO oxidation. By using a RF generated oxygen plasma and molecular beam techniques, details of CO oxidation with an oxygen precovered surface could be studied in UHV conditions and the role of metastable oxygen and water on surface reactivity was investigated.

Chapter 2 reports a gold study in which it was shown that CO reacts readily with pre-adsorbed oxygen atoms on a Au/TiO_2 planar model catalyst to produce CO_2 even at temperatures as low as 65 K, which points to a low activation energy for the reaction. Results were presented where gold particle size seemed to have little effect on the CO oxidation reaction when oxygen adatoms were pre-adsorbed on the surface. It was also shown that as the oxygen adatom coverage increases, the rate of CO oxidation decreases on Au/TiO_2 at cryogenic temperatures.

In Chapter 3, CO oxidation on oxygen precovered Au(111) was measured using molecular beam techniques at a sample temperature of 77 K as a function of oxygen coverage. Results were shown where prompt CO_2 production was seen when the CO beam impinges on the sample followed by an exponential decay of CO_2 production in all cases. At oxygen precoverages above 0.5 ML, the initial CO_2 production was shown to decrease with increasing oxygen precoverage mainly due to the decrease in CO uptake with increasing O precoverage. The reaction of CO oxidation at 77 K was suggested to follow a precursor mediated reaction mechanism, where CO is in a precursor state or trapped state and oxygen atoms are in a chemisorbed state.

Chapter 4 is a brief account of how water can promote oxidation of impinging CO molecules on an oxygen atom precovered Au(111) at low temperatures. CO_2 production was seen to greatly increase with the addition of water on the same oxygen precoverage, and it was proposed that these results were due to CO reacting directly with activated water or OH groups formed from water interacting with atomic oxygen on Au(111).

Chapter 5 deals with the details of Chapter 4 including the interaction of water and oxygen atoms on Au(111) surface. It was shown that water interacts with oxygen

atoms on the Au(111) surface resulting in oxygen scrambling on the surface. The role of metastable oxygen in the water-oxygen interaction and the promotion effect of water on CO oxidation on Au(111) are also discussed.

When molecular oxygen is used as an oxidant in heterogeneous catalysis, often times, water is overlooked as just a product molecule. In this dissertation, by demonstrating the promotional effect of water in CO oxidation on an oxygen covered Au(111) surface, water is brought to light as a key player in oxidation reactions.

It is likely that in real catalytic reactions under atmospheric conditions, molecular oxygen may form an oxygen transient that is much more reactive than stably chemisorbed oxygen on the surface. By artificially creating reactive oxygen on the surface and exploring various reactions, we can shed light on the true mechanism of chemical reactions occurring on real catalysts.

RECOMMENDATIONS FOR FUTURE RESEARCH

Molecular beam apparatus combined with a RF generated oxygen plasma source has been proven to be a very useful tool for investigating the mechanistic details of CO oxidation on gold catalysts and elucidating the function of metastable oxygen species in surface reactions. For future research, the generation of reactive oxygen on Au(111) can be utilized to examine other molecules that can donate acidic hydrogen to the reactive oxygen on the surface. Molecules such as methanol and ammonia are good candidates for studying the reactivity towards metastable oxygen species on the surface.

Recently, we acquired a metal cluster generator from Mantis which is equipped with magnetron sputtering unit and quadrupole mass selector. It can generate and deposit size selected metal particles on a planar metal oxide substrate. This will enable us to investigate the chemistry of nanometer sized metal particles of high melting point, which was not possible with our current evaporative metal doser. It is also capable of depositing bimetallic particles by using an appropriate metal target to generate metal particles of two components. We will begin by using Ir particles as our metal of choice on metal oxide substrates such as TiO_2 and SiO_2 and compare the results with our previous data on Ir single crystal surfaces. We can expand the methodology used in studying gold catalyst and investigate the particle size effect in various types of chemistry occurring on Ir particles supported by metal oxide substrates. An interesting property of Ir is that it has very favorable characteristics in ammonia decomposition. The desorption temperature of N_2 is relatively lower than other transition metals, thus decreasing the possibility of surface poisoning by nitrogen atoms.[3] This makes ammonia a good potential candidate for supplying hydrogen in alkaline fuel cell systems without poisoning the fuel cell electrodes by CO.[4] Normally, hydrocarbons are used as the source of hydrogen in many fuel cell applications. These hydrocarbon based fuel put out CO_x during the hydrogen production and CO generated in this process will deactivate the electrodes if untreated. Ir based catalysts can be used as an effective hydrogen producing unit without producing CO in the process. We can study the particle size effect of Ir in ammonia decomposition on different types of metal oxide supports and perhaps compare the reactivity with that of single crystal Ir.

Another interesting results regarding Ir is that epitaxially grown Au on Ir(111) seems to dissociate hydrogen.[5] This is very unusual since Au alone cannot dissociate hydrogen. It would be very interesting to grow Au on an Ir single crystal and repeat these experiments and investigate the adsorption behavior of other molecules such as oxygen in our apparatus and observe the outcome of this bimetallic system. What is more exciting about this topic is that since we are now able to grow size selected Ir particles on a planar substrate, we can subsequently vapor deposit Au on this surface and perhaps study the chemistry of core shell structure of Ir-Au system. And we can further compare these results with Ir-Au bimetallic clusters grown in a different way, such as using a bimetallic target to grow Ir-Au particles in the cluster generator. We will be able to compare these results of bimetallic catalysts with a metal oxide support with just Ir particles on the surface to observe the interesting chemistry on bimetal catalysts under UHV conditions.

REFERENCES

1. G. C. Bond, D. T. Thompson, Catal. Rev. – Sci. Eng. **41**, 319 (1999).

2. M. Haruta, Chem. Rec. **3**, 75 (2003).

3. A. K. Santra, B. K. Min, C. W. Yi, K. Luo, T. V. Choudhary, D. W. Goodman, J. Phys. Chem. B **106**, 340 (2002).

4. T. V. Choudhary, D. W. Goodman, Catal. Today **77**, 65 (2002).

5. M. Okada, M. Nakamura, K. Moritani, T. Kasai, Surf. Sci. **523**, 218 (2003).

Bibliography

H. M. Ajo, V. A. Bondzie, C. T. Campbell, Catal. Lett. **78**, 359 (2002).

D. Andreeva, V. Idakiev, T. Tabakova, L. Ilieva, P. Falaras, A. Bourlinos, A. Travlos, Catal. Today **72**, 51 (2002).

C. T. Au, A. F. Carley, A. Pashuski, S. Read, M. W. Roberts, A. Zeini-Isfahan, Springer Ser. Surf. Sci. **33**, 241 (1993).

C. T. Au, M. W. Roberts, Proc. Roy. Soc. London, Ser. A **396**, 165 (1984).

C. T. Au, M. W. Roberts, A. R. Zhu, J. Chem. Soc., Chem. Commun. 737 (1984).

G. R. Bamwenda, S. Tsubota, T. Nakamura, M. Haruta, Catal. Lett. **44**, 83 (1997).

K. Bange, T. E. Madey, J. K. Sass, E. M. Stuve, Surf. Sci. **183**, 334 (1987).

A. M. Baro, W. Erley, J. Vac. Sci. Technol. **20**, 580 (1982).

C. A. Becker, J. P. Cowin, L. Wharton, D. J. Auerbach, J. Chem. Phys. **67**, 3394 (1977).

K. Bedurftig, S. Volkening, Y. Wang, J. Wintterlin, K. Jacobi, G. Ertl, J. Chem. Phys. **111**, 11147 (1999).

J. Bergeld, B. Kasemo, D. V. Chakarov, Surf. Sci. **495**, L815 (2001).

F. Boccuzzi, A. Chiorino, J. Phys. Chem. B **104**, 5414 (2000).

F. Boccuzzi, A. Chiorino, M. Manzoli, P. Lu, T. Akita, S. Ichikawa, M. Haruta, J. Catal. **202**, 256 (2001).

M. A. Bollinger, M. A. Vannice, Appl. Catal. B: Environ. **8**, 417 (1996).

G. C. Bond, D. T. Thompson, Catal. Rev. – Sci. Eng. **41**, 319 (1999).

G. C. Bond, D. T. Thompson, Gold Bull. **33**, 41 (2000).

V. A. Bondzie, S. C. Parker, C. T. Campbell, Catal. Lett. **63**, 143 (1999).

H. G. Boyen, G. Kaestle, F. Weigl, B. Koslowski, C. Dietrich, P. Ziemann, J. P. Spatz, S. Riethmueller, C. Hartmann, M. Moeller, G. Schmid, M. G. Garnier, P. Oelhafen, Science **297**, 1533 (2002).

B. W. Callen, K. Griffiths, P. R. Norton, D. A. Harrington, J. Phys. Chem. **96**, 10905 (1992).

A. F. Carley, P. R. Davies in *Interfacial Science*, edited by M. W. Roberts (Blackwell, Oxford, 1997).

A. F. Carley, P. R. Davies, M. W. Roberts, N. Shukla, Y. Song, K. K. Thomas, Appl. Surf. Sci. **81**, 265 (1994).

A. F. Carley, P. R. Davies, M. W. Roberts, K. K. Thomas, Surf. Sci. **238**, L467 (1990).

S. Carrettin, P. McMorn, P. Johnston, K. Griffin, G. J. Hutchings, Chem. Commun. 696 (2002).

T. V. Choudhary, D. W. Goodman, Catal. Today **77**, 65 (2002).

J. R. Creighton, J. M. White, Surf. Sci. **136**, 449 (1984).

J. E. Crowell, J. G. Chen, D. M. Hercules, J. T. Yates, Jr., J. Chem. Phys. **86**, 5804 (1987).

S. T. Daniells, M. Makkee, J. A. Moulijn, Catal. Lett. **100**, 39 (2005).

M. Date, M. Haruta, J. Catal. **201**, 221 (2001).

M. Date, M. Okumura, S. Tsubota, M. Haruta, Angew. Chem. –Int. Edit. **43**, 2129 (2004).

P. R. Davies, M. W. Roberts, N. Shukla, D. J. Vincent, Surf. Sci. **325**, 50 (1995).

D. L. Doering, T. E. Madey, Surf. Sci. **123**, 305 (1982).

W. S. Epling, G. B. Hoflund, J. F. Weaver, S. Tsubota, M. Haruta, J. Phys. Chem. **100**, 9929 (1996).

R. M. Finch, N. A. Hodge, G. J. Hutchings, A. Meagher, Q. A. Pankhurst, M. R. H. Siddiqui, F. E. Wagner, and R. Whyman, Phys. Chem. Chem. Phys. **1**, 485 (1999).

G. B. Fisher, B. A. Sexton, Phys. Rev. Lett. **44**, 683 (1980).

Q. Fu, H. Saltsburg, M. Flytzani-Stephanopoulos, Science **301**, 935 (2003).

X.-Q. Gong, P. Hu, R. Raval, J. Chem. Phys. **119**, 6324 (2003).

J. M. Gottfried, Ph. D. thesis, the Freie Universität Berlin (2003).

J. M. Gottfried, K. J. Schmidt, S. L. M. Schroeder, K. Christmann, Surf. Sci. **525**, 197 (2003).

J.-D. Grunwaldt, A. Baiker, J. Phys. Chem. B **103**, 1002 (1999).

J.-D. Grunwaldt, M. Maciejewski, O.S. Becker, P. Fabrizioli, A. Baiker, J. Catal. **186**, 458 (1999).

B. Hammer, J. K. Nørskov, Nature **376**, 238 (1995).

J. Harris, B. Kasemo, Surf. Sci. **105**, L281 (1981).

M. Haruta, Catal. Today **36**, 153 (1997).

M. Haruta, Chem. Rec. **3**, 75 (2003).

M. Haruta, T. Kobayashi, H. Sano, N. Yamada, Chem. Lett. **16**, 405 (1987).

M. Haruta, S. Tsubota, T. Kobayashi, H. Kageyama, M. J. Genet, and B. Delmon, J. Catal. **144**, 175 (1993).

M. Haruta, N. Yamada, T. Kobayashi, and S. Iijima, J. Catal. **115**, 301 (1989).

T. Hayashi, K. Tanaka, M. Haruta, J. Catal. **178**, 566 (1998).

B. E. Hayden, M. E. Rendall, O. South, J. Am. Chem. Soc. **125**, 7738 (2003).

M. A. Henderson, Surf. Sci. Rep. **46**, 1 (2002).

H. T. Hess in *Kirk-Othmer Encyclopedia of Chemical Engineering*, edited by I. Kroschwitz, M. Howe-Grant (Wiley, New York, 1995).

N. A. Hodge, C. J. Kiely, R. Whyman, M. R. H. Siddiqui, G. J. Hutchings, Q. A. Pankhurst, F. E. Wagner, R. R. Rajaram, S. E. Golunski, Catal. Today **72**, 133 (2002).

M. D. Hughes, Y.-J. Xu, P. Jenkins, P. McMorn, P. Landon, D. I. Enache, A. F. Carley, G. A. Attard, G. J. Hutchings, F. King, E. H. Stitt, P. Johnston, K. Griffin, C. J. Kiely, Nature **437**, 1132 (2005).

P. Jiang, M. W. Zappone, S. L. Bernasek, A. Robertson, Jr., J. Vac. Sci. Technol. A **14**, 2372 (1996).

J. Kaspar, P. Fornasiero, N. Hickey, Catal. Today **77**, 419 (2003).

B. D. Kay, K. R. Lykke, J. R. Creighton, S. J. Ward, J. Chem. Phys. **91**, 5120 (1989).

T. S. Kim, J. D. Stiehl, C. T. Reeves, R. J. Meyer, C. B. Mullins, J. Am. Chem. Soc. **125**, 2018 (2003).

T. S. Kim, J. Gong, R. A. Ojifinni, J. M. White, C. B. Mullins, Manuscript in Preparation.

M. Klaua, T. E. Madey, Surf. Sci. **136**, L42 (1984).

K. Kretzschmar, J. K. Sass, P. Hofmann, A. Ortega, A. M. Bradshaw, S. Holloway, Chem. Phys. Lett. **78**, 410 (1981).

J. Kubota, J. Kondo, K. Domen, C. Hirose, Surf. Sci. **295**, 169 (1993).

G. U. Kulkarni, C. N. R. Rao, M. W. Roberts, Langmuir **11**, 2572 (1995).

X. Lai, T. P. St.Clair, M. Valden, D. W. Goodman, Prog. Surf. Sci. **59**, 25 (1998).

P. Landon, P. J. Collier, A. F. Carley, D. Chadwick, A. J. Papworth, A. Burrows, C. J. Kiely, G. J. Hutchings, Phys. Chem. Chem. Phys. **5**, 1917 (2003).

P. Landon, P. J. Collier, A. J. Papworth, C. J. Kiely, G. J. Hutchings, Chem. Commun. 2058 (2002).

M. A. Lazaga, D. T. Wickham, D. H. Parker, G. N. Kastanas, B. E. Koel, ACS Sym. Ser. **523**, 90 (1993).

T. Lei, M. S. Zei, G. Ertl, Surf. Sci. **581**, 142 (2005).

M. I. Lester, B. V. Pond, D. T. Anderson, L. B. Harding, A. F. Wagner, J. Chem. Phys. **113**, 9889 (2000).

S. D. Lin, M. Bollinger, M. A. Vannice, Catal. Lett. **17**, 245 (1993).

Z.-P. Liu, P. Hu, A. Alavi, J. Am. Chem. Soc. **124**, 14770 (2002).

Z.-P. Liu, S. J. Jenkins, D. A. King, Phys. Rev. Lett. **94**, 196102. (2005).

N. Lopez, J. K. Nørskov, J. Am. Chem. Soc. **124**, 11262 (2002).

N. Lopez, J. K. Nørskov, Surf. Sci. **515**, 175 (2002).

T. E. Madey, J. T. Yates, Jr., Chem. Phys. Lett. **51**, 77 (1977).

D. C. Meier, X. Lai, D. W. Goodman, in *Surface Chemistry and Catalysis*, edited by A. F. Carley (Kluwer Academic/Plenum Publishers, New York, 2002).

R. Meyer, C. Lemire, Sh. K. Shaikhutdinov, H.-J. Freund, Gold Bull. **37**, 72 (2004).

G. Mills, M. S. Gordon, H. Metiu, J. Chem. Phys. **118**, 4198 (2003).

G. Mul, A. Zwijnenburg, B. van der Linden, M. Makkee, J. A. Moulijn, J. Catal. **201**, 128 (2001).

C. B. Mullins, C. T. Rettner, D. J. Auerbach, J. Chem. Phys. **95**, 8649 (1991).

C. Nyberg, C. G. Tengstaal, J. Chem. Phys. **80**, 3463 (1984).

M. Okada, M. Nakamura, K. Moritani, T. Kasai, Surf. Sci. **523**, 218 (2003).

M. Okumura, S. Nakamura, S. Tsubota, T. Nakamura, M. Azuma, and M. Haruta, Catal. Lett. **51**, 53 (1998).

D. A. Outka, R. J. Madix, J. Am. Chem. Soc. **109**, 1708 (1987).

D. A. Outka, R. J. Madix, Surf. Sci. **179**, 351 (1987).

T. Pache, H. P. Steinrueck, W. Huber, D. Menzel, Surf. Sci. **224**, 195 (1989).

D. H. Parker, B. E. Koel, J. Vac. Sci. Technol. A **8**, 2585 (1990).

J. E. Pollard, Rev. Sci. Instrum. **63**, 1771 (1992).

T. Rockmann, C. A. M. Brenninkmeijer, G. Sauerssig, P. Bergamaschi, J. N. Crowley, H. Fischer, P. J. Cruutzen, Science **281**, 544 (1998).

N. Saliba, D. H. Parker, B. E. Koel, Surf. Sci. **410**, 270 (1998).

A. K. Santra, B. K. Min, C. W. Yi, K. Luo, T. V. Choudhary, D. W. Goodman, J. Phys. Chem. B **106**, 340 (2002).

M. M. Schubert, S. Hackenberg, A. C. van Veen, M. Muhler, V. Plzak, R. J. Behm, J. Catal. **197**, 113 (2001).

M. Schulze, R. Reissner, K. Bolwin, W. Kuch, Fresen. J. Anal. Chem. **353**, 661 (1995).

B. Schumacher, V. Plzak, M. Kinne, R. J. Behm, Catal. Lett. **89**, 109 (2003).

A. P. Seitsonen, Y. Zhu, K. Beduerftig, H. Over, J. Am. Chem. Soc. **123**, 7347 (2001).

Y. Shao, J. Paul, Appl. Surf. Sci. **72**, 113 (1993).

A. Spitzer, H. Lueth, Surf. Sci. **160**, 353 (1985).

E. E. Stangland, K. B. Stavens, R. P. Andres, W. N. Delgass, J. Catal. **191**, 332 (2000).

J. D. Stiehl, T. S. Kim, S. M. McClure, C. B. Mullins, J. Am. Chem. Soc. **126**, 1606 (2003).

J. D. Stiehl, T. S. Kim, S. M. McClure, C. B. Mullins, J. Am. Chem. Soc. **126**, 13574 (2004).

J. D. Stiehl, T. S. Kim, C. T. Reeves, R. J. Meyer, C. B. Mullins, J. Phys. Chem. B **108**, 7917 (2004).

T. Sueyoshi, T. Sasaki, Y. Iwasawa, J. Phys. Chem. B **101**, 4648 (1997).

P. A. Thiel, F. M. Hoffmann, W. H. Weinberg, Phys. Rev. Lett. **49**, 501 (1982).

S. Tsubota, D. A. H. Cunningham, Y. Bando, M. Haruta, Stud. Surf. Sci. Catal. **91**, 227 (1995).

A. Ueda, M. Haruta, Gold Bull. **32**, 3 (1999).

B. S. Uphade, T. Akita, T. Nakamura, M. Haruta, J. Catal. **209**, 331 (2002).

M. Valden, X. Lai, D. W. Goodman, Science **281**, 1647 (1998).

M. Valden, S. Pak, X. Lai, D. W. Goodman, Catal. Lett. **56**, 7 (1998).

M. C. Wheeler, C. T. Reeves, D. C. Seets, C. B. Mullins, J. Chem. Phys. **108**, 3057 (1998).

M. C. Wheeler, D. C. Seets, C. B. Mullins, J. Chem. Phys. **105**, 1572 (1996).

M. C. Wheeler, D. C. Seets, C. B. Mullins, J. Chem. Phys. **107**, 1672 (1997).

Y. Xu, M. Mavrikakis, J. Phys. Chem. B **107**, 9298 (2003).

Vita

Tae Sang Kim was born in Seoul, Korea on November 26, 1973, the son of Hye Sook Park and Moo Sung Kim. In 1993, after graduating from Yang Jae High School in Seoul, Korea, he enrolled in Seoul National University in Seoul, Korea. After two years of study at Seoul National University, he served in the Republic of Korea Air Force for 30 months. He returned to school in 1998 and completed his Bachelor of Science in Chemical Engineering in February 2000. He began his graduate education at the University of Texas at Austin in September 2000.

Permanent address: 3500 Greystone Dr. #239, Austin, TX 78731

This dissertation was typed by the author.